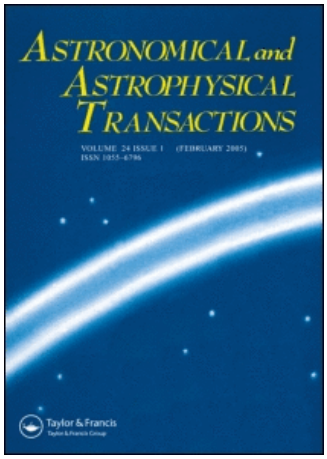

Astronomical & Astrophysical Transactions
The Journal of the Eurasian Astronomical Society
Publication details, including instructions for authors and subscription information:
http://www.informaworld.com/smpp/title~content=t713453505

Coordinated observations of the red dwarf flare star EV LAC in 1994 and 1995

E. P. Abranin [a]; I. Yu. Alekseev [b]; S. Avgoloupis [c]; L. L. Bazelyan [a]; S. V. Berdyugina [b]; G. Cutispoto [d]; R. E. Gershberg [b]; V. M. Larionov [e]; G. Leto [f]; V. N. Lisachenko [a]; G. Marino [d]; L. N. Mavridis [c]; S. Messina [d]; V. N. Mel'nik [a]; I. Pagano [d]; S. V. Pustil'nik [g]; M. Rodonò [d]; G. Sh. Roizman [g]; J. H. Seiradakis [c]; G. P. Sigal [g]; N. I. Shakhovskaya [b]; D. N. Shakhovskoy [b]; V. A. Shcherbakov [b]
[a] Institute of Radio Astronomy, National Academy of Sciences of Ukraine, Kharkov, Ukraine
[b] Crimean Astrophysical Observatory, Crimea, Ukraine
[c] Department of Physics, Section of Astrophysics, Astronomy and Mechanics, University of Thessaloniki, Thessaloniki, Greece
[d] Astrophysical Observatory and Institute of Astronomy of Catania University, Catania, Italy
[e] Astronomical Institute of the St.-Petersburg University, St.-Petersburg, Russia
[f] CNR Radio Astronomy Institute, Italy
[g] Sea of Galilee Astrophysical Observatory, Jordan Valley Academic College, Israel

Online Publication Date: 01 March 1998
To cite this Article: Abranin, E. P., Alekseev, I. Yu., Avgoloupis, S., Bazelyan, L. L., Berdyugina, S. V., Cutispoto, G., Gershberg, R. E., Larionov, V. M., Leto, G., Lisachenko, V. N., Marino, G., Mavridis, L. N., Messina, S., Mel'nik, V. N., Pagano, I., Pustil'nik, S. V., Rodonò, M., Roizman, G. Sh., Seiradakis, J. H., Sigal, G. P., Shakhovskaya, N. I., Shakhovskoy, D. N. and Shcherbakov, V. A. (1998) 'Coordinated observations of the red dwarf flare star EV LAC in 1994 and 1995', Astronomical & Astrophysical Transactions, 17:3, 221 - 262
To link to this article: DOI: 10.1080/10556799808232093
URL: http://dx.doi.org/10.1080/10556799808232093

Astronomical and Astrophysical Transactions, 1998, Vol. 17, pp. 221–262
Reprints available directly from the publisher
Photocopying permitted by license only

COORDINATED OBSERVATIONS OF THE RED DWARF FLARE STAR EV LAC IN 1994 AND 1995

E. P. ABRANIN[1], I. Yu. ALEKSEEV[2], S. AVGOLOUPIS[3], L. L. BAZELYAN[1], S. V. BERDYUGINA[2], G. CUTISPOTO[4], R. E. GERSHBERG[2], V. M. LARIONOV[5], G. LETO[6], V. N. LISACHENKO[1], G. MARINO[4], L. N. MAVRIDIS[3], S. MESSINA[4], V. N. MEL'NIK[1], I. PAGANO[4], S. V. PUSTIL'NIK[7], M. RODONÒ[4], G. Sh. ROIZMAN[7], J. H. SEIRADAKIS[3], G. P. SIGAL[7], N. I. SHAKHOVSKAYA[2], D. N. SHAKHOVSKOY[2], and V. A. SHCHERBAKOV[2]

[1] *Institute of Radio Astronomy, National Academy of Sciences of Ukraine, Kharkov, Ukraine*
[2] *Crimean Astrophysical Observatory, Nauchny, Crimea, Ukraine*
[3] *University of Thessaloniki, Department of Physics, Section of Astrophysics, Astronomy and Mechanics, GR-54006, Thessaloniki, Greece*
[4] *Astrophysical Observatory and Institute of Astronomy of Catania University, I-95125 Catania, Italy*
[5] *Astronomical Institute of the St.-Petersburg University, St.-Petersburg, Russia*
[6] *CNR Radio Astronomy Institute, Noto VLBI Station, Italy*
[7] *Sea of Galilee Astrophysical Observatory, Jordan Valley Academic College, Jordan Valley, 15132, Israel*

(Received October 8, 1997)

The results of photometric, spectral and radio studies of the flare star EV Lac we obtained during the course of cooperative observations in 1994 and 1995 are presented. A quantitative analysis of the radiation emitted by two powerful flares using the colour–colour diagram confirms the previous conclusion on the essential heterogeneity of matter radiating in optical flares. From simultaneous observations of the star in *UBVRI*, *K* and *H* bands no significant brightness variations in IR were found in coincidence with observed small-amplitude optical flares, except a gradual decrease in the *K*-band following a 1.0 mag flare in the *U*-band. A differential spottedness of bright and dark hemispheres of EV Lac is estimated using observations in separate seasons and the total stellar spottedness is determined within the framework of the zonal spottedness model. Spectra of quiet and active states of the star in the blue-green region in 1994 and in the red region in 1995 are described: the characteristics of the quiet chromosphere in the H_α, H_β, H_γ lines, their widening during flares, the strengthening of neutral helium lines and the appearance of emission lines of He II and metals are presented. The monitoring of EV Lac in decametric wavelengths with the largest radio telescope UTR-2 led to the detection of 18 radio bursts, one of which satisfies the majority of criteria of signals of non-terrestrial origin and coincides in time with an optical flare.

KEY WORDS Stars: flare – stars: individual: EV Lac – radiation mechanism: non thermal – stars: activity

1 INTRODUCTION

From August 26 to August 31, 1994, and from August 30 to September 4, 1995, two campaigns of cooperative observations of the flare red dwarf star EV Lac were undertaken. As in previously described similar campaigns (Gershberg *et al.*, 1991a,b; Berdyugin *et al.*, 1995; Gershberg *et al.*, 1993; Alekseev *et al.*, 1994; Abdul-Aziz *et al.*, 1995), the task of the cooperative observations was to obtain long-duration series of homogeneous photometric data for EV Lac, which is one of the brightest and most active objects among the UV Cet type stars, and to obtain simultaneous photometry and other types of observations – spectral, infrared and radio, for which the availability of synchronous photometry is essential. In this paper we describe in detail the observations and the data obtained during these two campaigns.

2 PHOTOMETRY AND COLORIMETRY

2.1 Observations and General Results

The overall temporal coverage of EV Lac by observations, achieved in the international campaigns of 1994 and 1995, is presented in Figure 1. The times of brightness maxima of flares are marked by vertical lines, their lengths corresponding to the amplitudes of flares measured in stellar magnitudes.

In the Crimea the photometric monitoring was carried out by I. Yu. Alekseev with the *UBVRI* photometer–polarimeter described by Piirola (1984) and installed on the 1.25 m reflector AZT-11. The *U*-band light curves of the star obtained during these observations are shown in Figure 1. In Table 1 the quantitative characteristics of the registered flares are listed: times of brightness maxima, durations of flare rise (T_b) and of flare decay (T_a), flare equivalent durations $P = \int[(I_f - I_0)/I_0]\,dt$, I_f and I_0 being the count rates during the flare and out of the flare respectively, amplitudes of flares ΔU above $U_0 = 12\overset{m}{.}9$, colour indices $U-B$, $B-V$, $V-R$ and $V-I$ of pure flare radiation at brightness maxima.

In 1994 during 32.3 hours of patrol observations in Crimea 20 flares were registered and the ratio $\frac{\Sigma P_U}{T}$ where T is the total duration of monitoring, was 0.075; in 1995 during 34.4 hours 22 flares were registered and the ratio $\frac{\Sigma P_U}{T}$ was 0.015.

At the Stephanion Observatory of the University of Thessaloniki, Greece, EV Lac was monitored by S. Avgoloupis, L. N. Mavridis and J. H. Seiradakis with the 30-inch reflector in the *B*-band. The telescope, its photometric system and technique of observations were described earlier (Mavridis *et al.*, 1982).

In 1994 the observations in Greece were carried out during nine nights – from August 25 to September 2. Three nights – August 25 and September 1 and 2 – were outside the interval of cooperative observations. During the total of 29^h15^m patrol times 17 flares were registered, including 9^h37^m monitoring during the additional nights with eight flares detected. In Table 2, which is similar to Table 1, the quantitative characteristics of all flares registered in Greece are tabulated. In Figu-

Table 1. Quantitative characteristics of flares registered in Crimea

Date and UT of brightness maxima				T_b *min*	T_a *min*	P *min*	ΔU *mag*	$U-B$ *mag*	$B-V$ *mag*	$V-R$ *mag*	$V-I$ *mag*
1994											
26.08.	22^h	07^m	54^s	0.6	3.5	1.0	0.47				
28.08.	18	30	31	0.8	2.0	1.6	1.32	-1.04 ± 0.06	-0.05 ± 0.15	1.03 ± 0.19	
	18	47	42	0.4	16.9	7.2	0.82	-0.84 ± 0.09	0.00 ± 0.24		
	19	17	01	1.1	7.3	2.1	0.71	-0.98 ± 0.11			
	23	02	57		5.0	2.1	0.64				
	23	31	43	2.6	7.2	61.7	3.60				
29.08.	20	31	23	0.6	2.5	0.4	0.33				
	20	39	03	0.6	9.7	9.0	1.05	-0.86 ± 0.07	-0.37 ± 0.21		
	21	39	03	1.5	14.3	3.2	0.47	-0.61 ± 0.20			
30.08.	19	30	33	0.9	22.8	8.7	1.14	-1.19 ± 0.07	-0.47 ± 0.23		
	23	18	48	0.6	5.3	1.6	0.85	-0.88 ± 0.09	-0.34 ± 0.26		
	23	29	38	0.4	2.5	0.3	0.27				
31.08.	18	45	09	0.4	8.0	3.7	1.38	-0.80 ± 0.05	0.02 ± 0.11	0.80 ± 0.21	
	19	39	45	0.8	3.8	0.6	0.42				
	20	46	11	4.8	33.5	14.1	0.94	-0.94 ± 0.09	-0.27 ± 0.20		
	21	21	41	1.1	29.0	11.4	1.29	-0.92 ± 0.09	-0.41 ± 0.21		
	23	23	37	0.9	12.2	10.5	1.83	-0.72 ± 0.02	0.06 ± 0.05	0.50 ± 0.09	0.32 ± 0.15
	24	04	06	0.7	7.0	1.5	0.56	-1.16 ± 0.18			
	24	53	03	3.5	8.5	3.0	0.34	-0.78 ± 0.23			
	25	37	29	3.2	4.3	1.7	0.38				
1995											
31.08.	18	37	24	3.0	6.5	1.14	0.54				
	19	32	12	3.0	4.0	1.18	0.33				
	21	13	03	0.4	12.0	1.82	0.38				
	22	25	01	6.0	13.8	2.72	0.47				
	22	42	01	0.9	3.0	0.40	0.20				
	23	16	26	0.6	2.9	0.51	0.45				
	23	32	52	0.6	2.0	0.10	0.14				
	25	06	43	1.3	15.5	2.05	0.20				
02.09.	18	45	11	0.4	5.1	1.73	0.67				
	19	02	40	3.0	4.0	1.01	0.25				
	21	33		clouds							
03.09.	17	30		clouds							
	18	48	59	0.9	9.0	9.20	2.13	-0.91 ± 0.03	-0.02 ± 0.06	0.40 ± 0.10	0.49 ± 0.15
	20	35	14	1.9	8.3	0.98	0.22				
	21	01	00	0.5	2.6	0.23	0.22				
	21	29	13	2.6	16.5	4.05	0.45				
	23	45	40	0.2	1.5	0.21	0.46				
04.09.	18	02	30	clouds			1.10				
	21	18	47	0.9	6.0	0.77	0.34				
	21	54	35	0.7	3.0	0.21	0.15				
	23	26	19	0.6	11.0	1.10	0.22				
	25	23	25	0.8	5.5	0.75	0.22				

re 3 B-band light curves of the strongest flares with $\Delta B > 0.5$ mag are given for the events additional to Figure 2.

In 1995 at the Stephenion Observatory the observations were carried out from August 28 to September 6. During a total of 23^h15^m monitoring time three strong

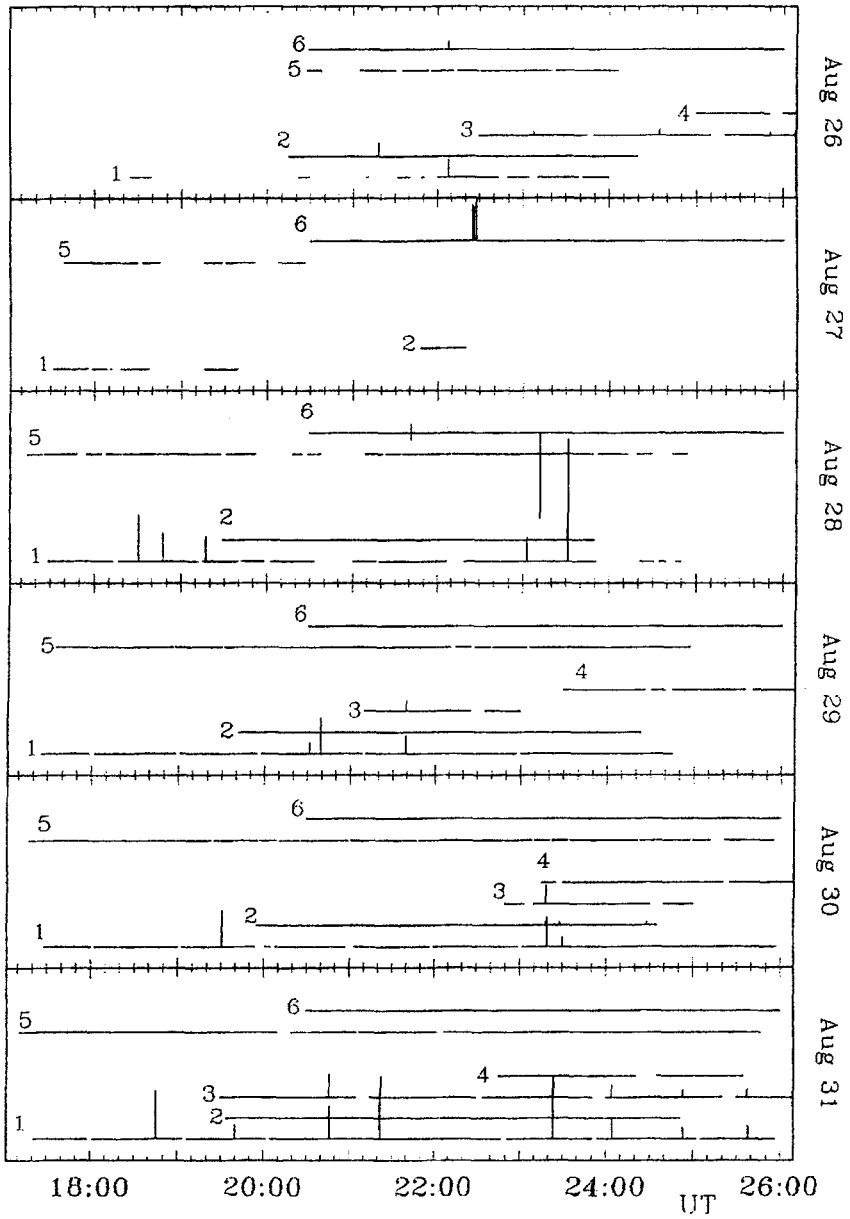

Figure 1a The temporal distribution of patrol observations of EV Lac in 1994: 1, *UBVRI photometric patrol in Crimea*; 2, *B-band photometry in Greece*; 3, *UBV monitoring in Italy*; 4, *K*-band monitoring in Italy; 5, spectral observations at the Shajn reflector in Crimea; 6, radio monitoring in the decametric wavelength range in Kharkov; times of optical flare maxima, are indicated by vertical lines, their lengths are proportional to the flare amplitudes measured in stellar magnitudes; radio bursts are also marked by vertical lines which are directed upward for the 20 MHz and downward for the 25 MHz observations.

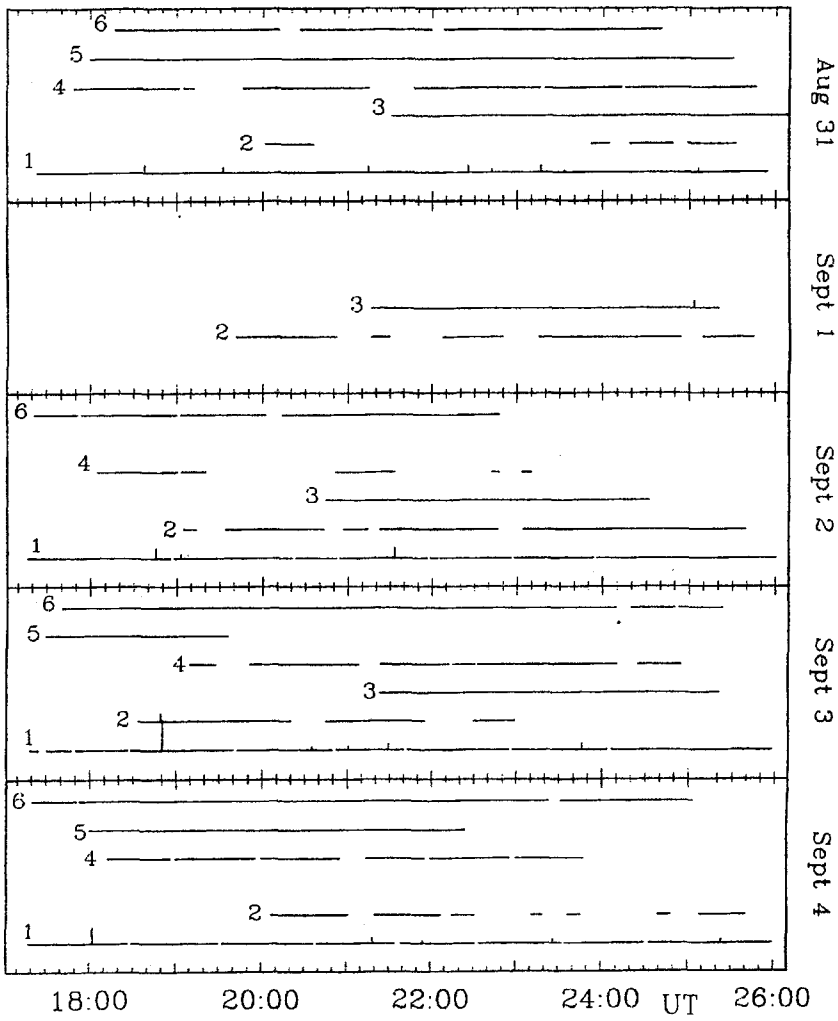

Figure 1b The same as Figure 1a for 1995: 1, *UBVRI* photometric patrol in Crimea; 2, *B*-band photometry in Greece; 3, *UBV* and *K* photometry in Italy; 4, IR patrol in Crimea; 5, *BVR* photometry in Israel; 6, spectral observations in Crimea.

flares with $\Delta B > 0.5$ mag were detected, two of which – on 29.8.95 UT 21:19 and on 5.9.95 UT 22:27 – were registered during 5^h47^m observations undertaken during nights, lying outside the cooperative programme. Characteristics of these flares are included in Table 2 and in Figure 3.

At the mountain station of the Catania Astrophysical Observatory on Mt. Etna (Italy), G. Cutispoto, G. Leto, G. Marino, S. Messina, I. Pagano and M. Rodonò carried out a photometric patrol of EV Lac in 1994 with two telescopes: the 80-cm automatic photoelectric telescope in the *UBV* bands and the 91-cm reflector

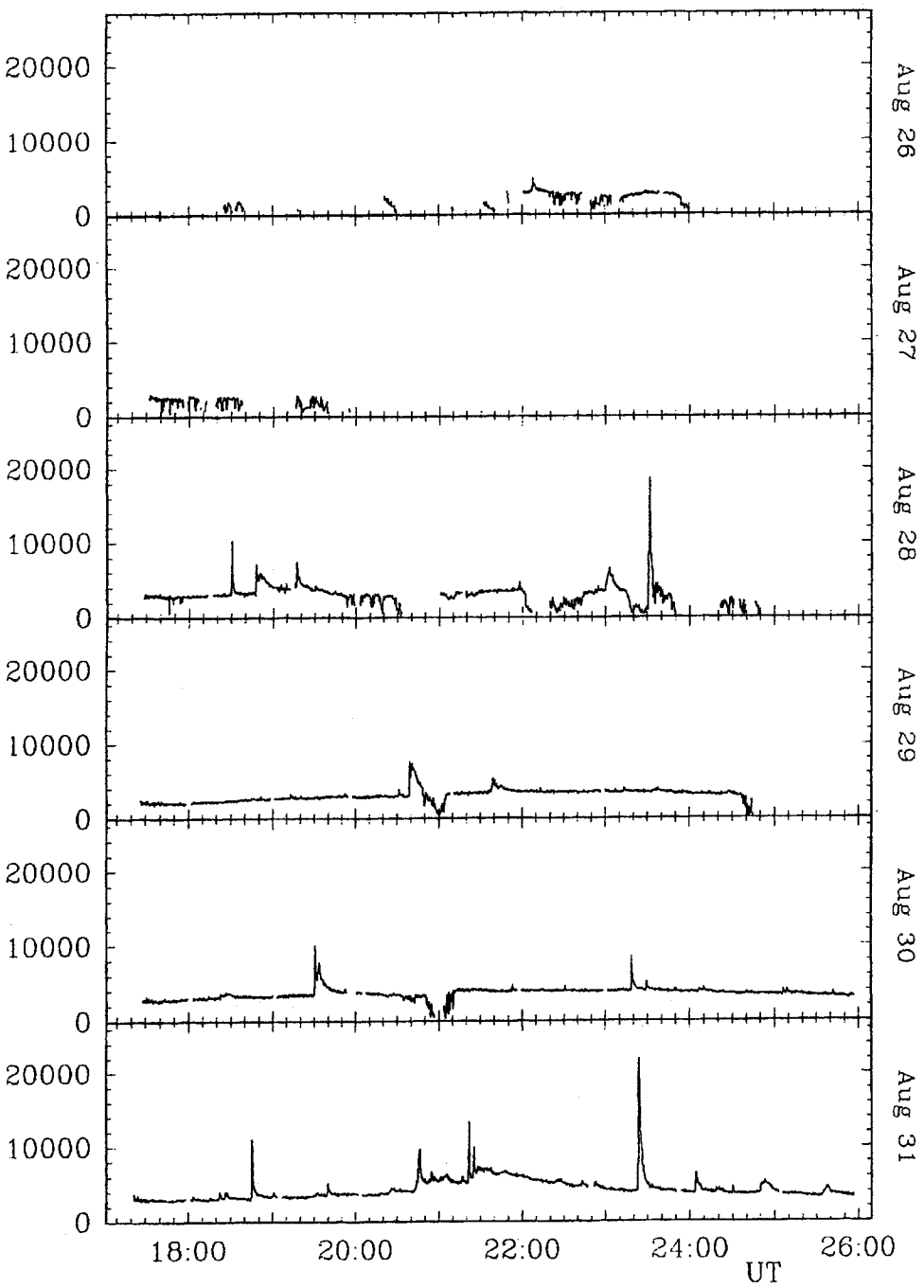

Figure 2a *U*-band light curves of EV Lac, registered in Crimea, in 1994.

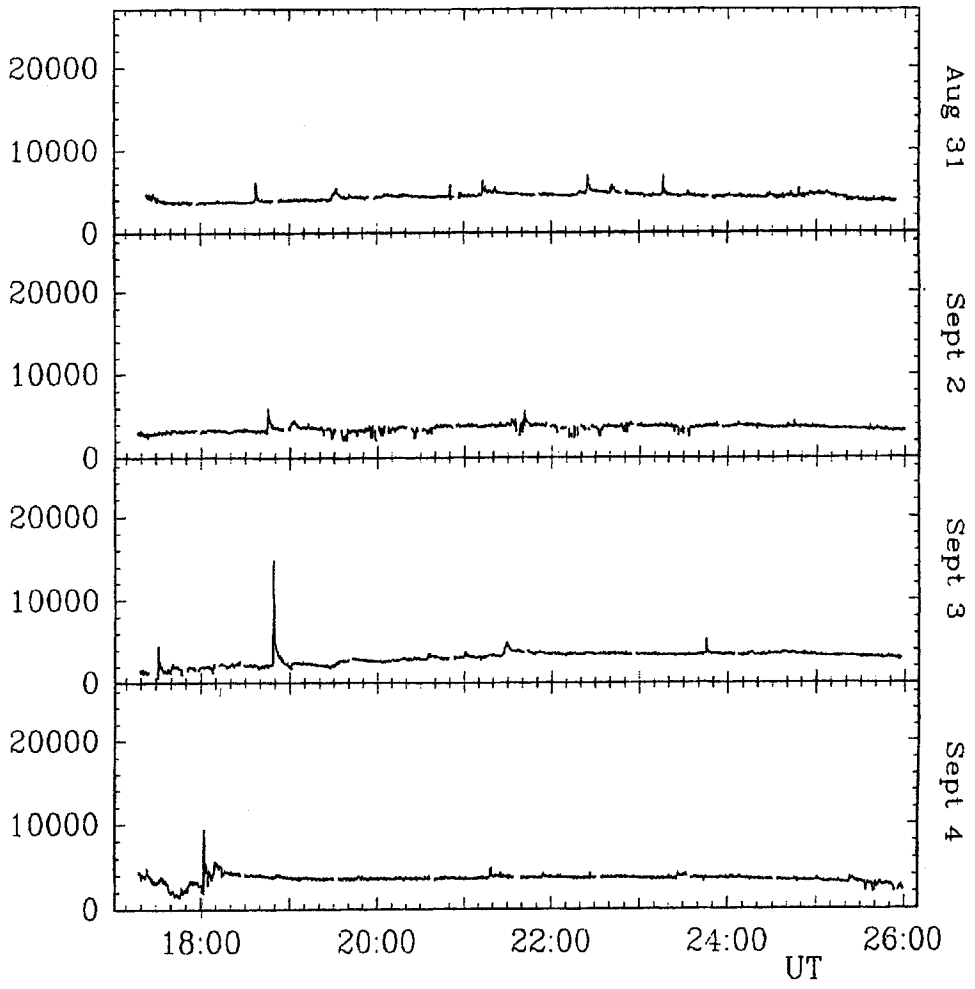

Figure 2b The same as Figure 2a for 1995.

in the near IR K-band. Observations were performed during nine nights, five of which were additional to the schedule of the cooperative programme. The times of brightness maxima, amplitudes and equivalent durations of flares registered in the UBV bands are presented in Table 3. The K-band monitoring took place during six optical flares with amplitudes ΔU from 0.5 mag up to 2.0 mag, but only during one of them – the flare on 3.9.94 at UT 24:27 with amplitude $\Delta U = 1.0$ mag – one may suggest some effect on the K-band light curve: a gradual decrease of the stellar brightness over 20–30 min after the optical flare decay – see Figure 4.

At the same site UBV observations were done in 1995 during six nights from August 30 to September 5. Due to windy weather conditions only 2^h53^m of coverage

Table 2. Quantitative characteristics of flares registered in Greece

Date and UT of brightness maxima	T_b *min*	T_a *min*	P_B *min*	ΔB *mag*
1994				
26.08 $21^h\ 18.2^m$	0.40	5.62	1.03	0.98
28.08 23 02.8	1.32	5.60	0.38	0.18
28.08 23 31.5	5.12	12.28	2.85	0.80
29.08 20 39.0	0.28	9.72	0.86	0.22
30.08 23 18.5	0.28	4.40	0.17	0.16
31.08 00 27.6	0.04	3.50	0.08	0.18
31.08 20 45.3	0.24	2.16	0.16	0.16
31.08 21 21.6	1.52	4.73	0.17	0.21
31.08 23 24.1	1.60	6.80	1.21	0.56
01.09 < 20 18.3		> 19.1	> 2.45	> 0.44
01.09 21 12.6	1.52	1.98	0.14	0.13
01.09 21 32.7	1.34	1.90	0.15	0.12
01.09 21 49.9	1.26	3.60	0.21	0.13
01.09 22 21.0	1.84	4.36	0.17	0.10
02.09 19 48.8	0.90	4.40	0.15	0.14
02.09 21 27.2	0.59	18.6	3.20	1.28
02.09 22 42.8	2.32	4.58	0.60	0.35
1995				
29.08 21 19.1	2.38	51.3	7.66	0.77
03.09 18 47.7	0.72	15.7	1.30	0.55
05.09 22 26.6	0.16	0.36	0.21	0.62

were secured. No flares of amplitude greater than 0.06 mag in the U-band were observed, exept the flare recorded on September 1 at 25:03 UT (see Table 3). Since the descent phase of this event was missed, a lower limit for the equivalent duration was computed. The K-band monitoring in 1995 was secured during four nights, from August 30 to September 3. No significant variability ($\sigma(K) = 0.025$ mag) was found during the total of 5^h54^m of coverage.

In 1995 during four nights V. M. Larionov carried out IR monitoring of EV Lac, using the 70-cm telescope AZT-8 of the Crimean Astrophysical Observatory and the IR photometer of the Astronomical Institute of the St.Petersburg University with an InSb detector, cooled by liquid nitrogen. Taking into account results of the IR monitoring of EV Lac in 1994 in the K-band, when no essential changes were found during optical flares, the H-band (1.62 μm) was selected for observations in 1995. In particular, the choice of the H-band was stimulated with the location of the H^- opacity maximum there. The observations were carried out with 24 s integration time. The error of an individual measurement was about 0.03 mag. The intervals of simultaneous recordings of EV Lac in the U and H bands are shown in Figure 5. During the simultanious monitoring in the optical and IR ranges, eight small flares with ΔU amplitudes of 0.2 mag up to 0.5 mag were registered. However, no significant brightness increase or decrease in the H band was found in any case, as expected in the case of small-amplitude flares, according to some current stellar flare models.

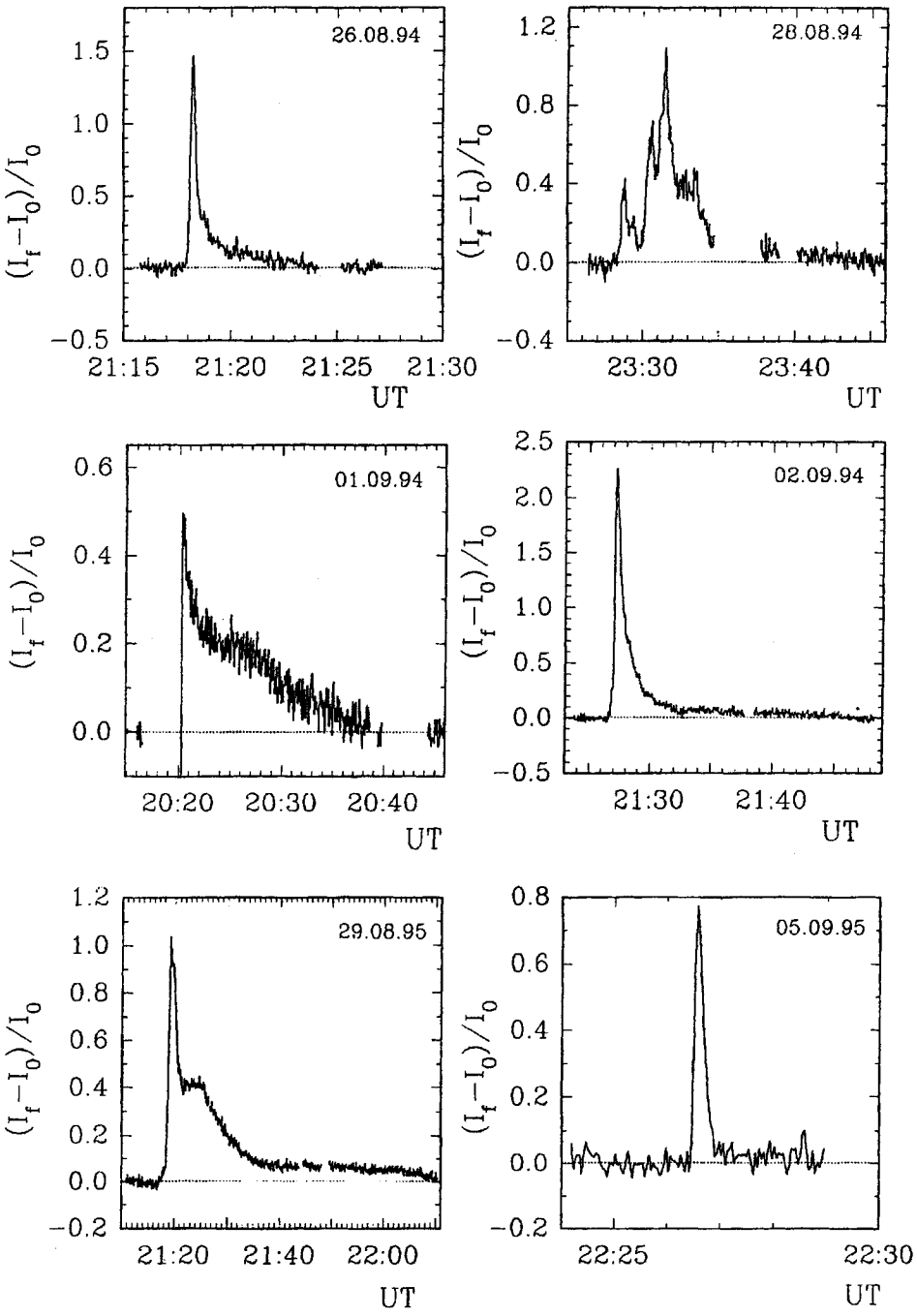

Figure 3 *B*-band light curves of EV Lac detected in Greece. The time resolution was 2.4 s.

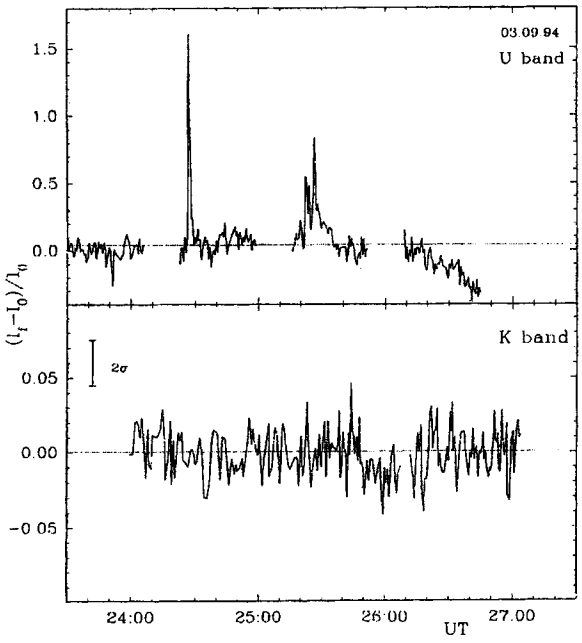

Figure 4 Fragments of the EV Lac light curves in the U and K bands, registered simultaneously in Catania, during flares detected in the U-band.

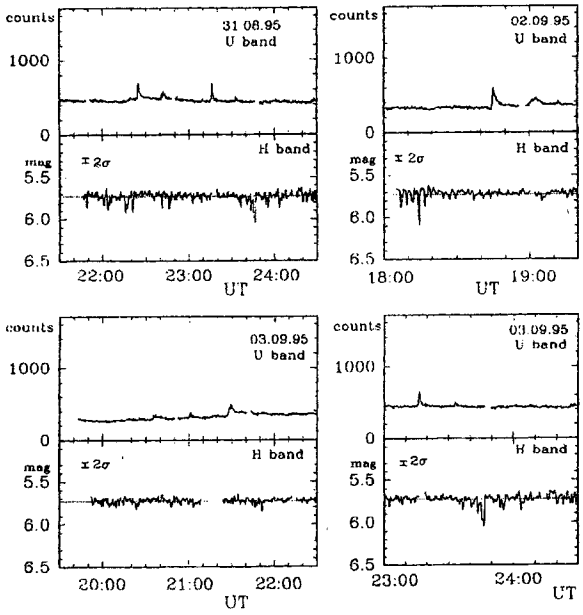

Figure 5 Fragments of the EV Lac light curves in the U and H bands, registered simultaneously in Crimea.

Table 3. Quantitative characteristics of flares registered in Catania

Date and UT of brightness maxima				ΔU *mag*	P_U *min*	ΔB *mag*	P_B *min*	ΔV *mag*	P_V *min*
1994									
26.08	23^h	08^m	38^s	0.31 ± 0.04	0.96				
26.08	24	35	36	0.52 ± 0.04	1.35	0.19 ± 0.04	0.38		
29.08	21	39	29	0.57 ± 0.04	3.37				
30.08	23	17	56	0.89 ± 0.06	1.58	0.16 ± 0.03	0.14	0.07 ± 0.03	0.14
31.08	20	46	16	1.41 ± 0.01	20.4				
31.08	21	22	07	1.23 ± 0.01	73.1	0.21 ± 0.04	4.09	0.16 ± 0.05	3.55
31.08	23	23	57	2.05 ± 0.01	13.0	0.65 ± 0.02	1.87	0.25 ± 0.04	0.43
31.08	24	04	24	0.59 ± 0.02	1.76				
31.08	24	56	23	0.43 ± 0.03	2.12				
31.08	25	37	34	0.48 ± 0.03	6.95	0.07 ± 0.04	0.30		
1.09	20	17	51	1.82 ± 0.01	40.4	0.63 ± 0.01	5.91	0.28 ± 0.02	3.21
1.09	22	21	07	1.22 ± 0.02	192.5	0.34 ± 0.01	44.0	0.14 ± 0.02	7.46
1.09	26	30	05	1.35 ± 0.02	8.53	0.33 ± 0.01	1.13	0.13 ± 0.02	0.18
2.09	21	27	48	3.10 ± 0.01	28.9	1.18 ± 0.01	4.11	0.61 ± 0.01	1.04
2.09	23	05	34	0.51 ± 0.05	1.79	0.14 ± 0.02	1.75		
2.09	24	10	48	1.23 ± 0.02	88.4	0.34 ± 0.02	14.2	0.07 ± 0.02	2.84
3.09	24	26	45	1.03 ± 0.02	2.11	0.37 ± 0.01	1.05	0.07 ± 0.02	0.18
3.09	25	26	22	0.65 ± 0.02	4.21	0.10 ± 0.01	0.53	0.06 ± 0.02	0.40
10.09	25	31	10	0.39 ± 0.05	0.41				
10.09	25	51	20	0.46 ± 0.05	1.25				
1995									
1.09	25	02	53	0.69 ± 0.06	≥ 10.8	$0.12 + 0.04$	≥ 0.84	≤ 0.03	

2.2 Analysis of Colour Indices of Pure Flare Radiation

Among the 42 flares, listed in Table 1, two were strong enough that it was possible to estimate all colour indices of pure flare radiation with sufficient accuracy. These were the flares observed on 31.8.94 at UT 23:24 and on 3.9.95 at UT 18:49, for which the errors of each of the four colour indices of the *UBVRI* system do not exceed 0.15 mag near brightness maxima. The technique of the analysis of such powerful flares with colour–colour diagrams for pure flare radiation has been described earlier (Alekseev *et al.*, 1994; Abdul-Aziz *et al.*, 1995).

In Figure 6 the U-band light curves and colour index curves are given for the above mentioned powerful flares. Numbered vertical dashed lines mark characteristic points on the light curves, which were chosen for the colourimetric analysis. On the light curve of the flare on 31.8.94 point 1 is at the premaximum phase of the flare, points 2 and 3 are located at the main and secondary brightness maxima and point 4 is the last point on the descending branch of the light curve, where all four colour indices can be measured with a sufficient degree of accuracy. On the light curve of the flare on 3.9.95, point 5 is at the brightness maximum and point 6 is similar to point 4 in the previous flare.

In Figure 7 numbered rectangles, whose numbering corresponds to points in Figure 6 and whose sizes correspond to the errors of determination of the respective

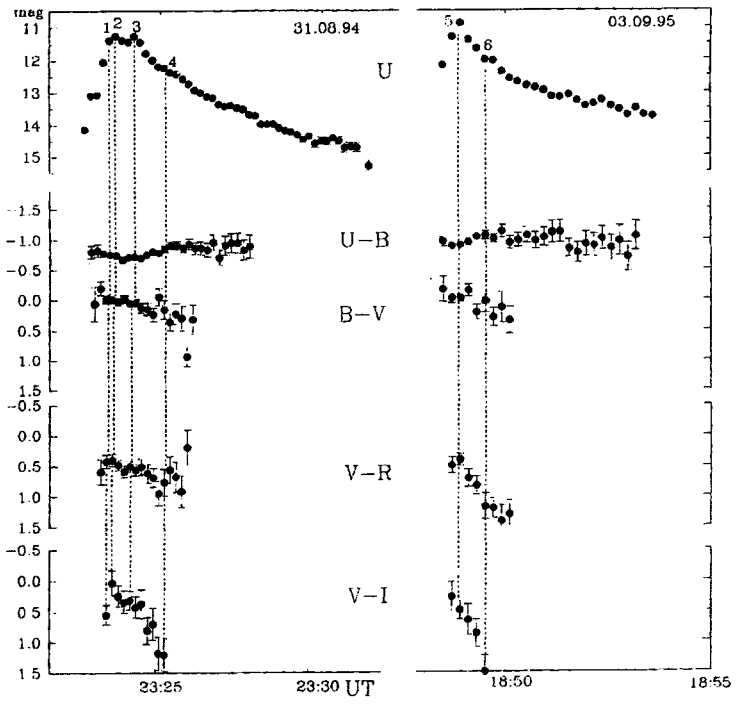

Figure 6 Light and colour indices curves of two strong flares, registered in the *UBVRI* system in Crimea on 31.8.94 and 3.9.95; in the quiet state the star has $U = 12^{\rm m}.9$, $U-B = 1^{\rm m}.1$, $B-V = 1^{\rm m}.6$, $V-R = 1^{\rm m}.8$ and $V-I = 3^{\rm m}.2$.

colour indices, mark the pure flare radiation location on the colour–colour diagrams. The locations of several known emission mechanisms mentioned in the caption of Figure 7 are also given by geometric curves. Comparing these data with the observations, it is possible to draw some conclusions concerning the physical nature of flare radiation.

As well as in earlier investigated powerful flares (Alekseev *et al.*, 1994; Abdul-Aziz *et al.*, 1995), taking a close look at the $(U-B, B-V)$ diagram, one notes that flare radiation at the brightness maxima – rectangles 2,3 and 5 – close enough to the *black body* radiation. The flare radiation shortly before the brightness maximum – rectangle 1 – can also be explained by the same mechanism. The $(U-B, V-R)$ diagram indicates that this flare radiation is shifted from the *black body* line toward the regions of *hydrogen plasma* or *layers of stellar atmosphere heated up by fluxes of fast particles.* The $(B-V, V-R)$ diagram shows that the alternative, proposed by the previous diagram, should be solved in favour of *plasma radiation.* Finally, the situation does not seem to be clarified by the $(U-B, V-I)$ index: in the $(U-B, V-I)$ diagram the flare radiation during the brightness maxima covers a very wide area, occupied by all considered mechanisms of emission. Passing to the colour indices of the flare fading phase – rectangles 4 and 6 – we find shifts of flare

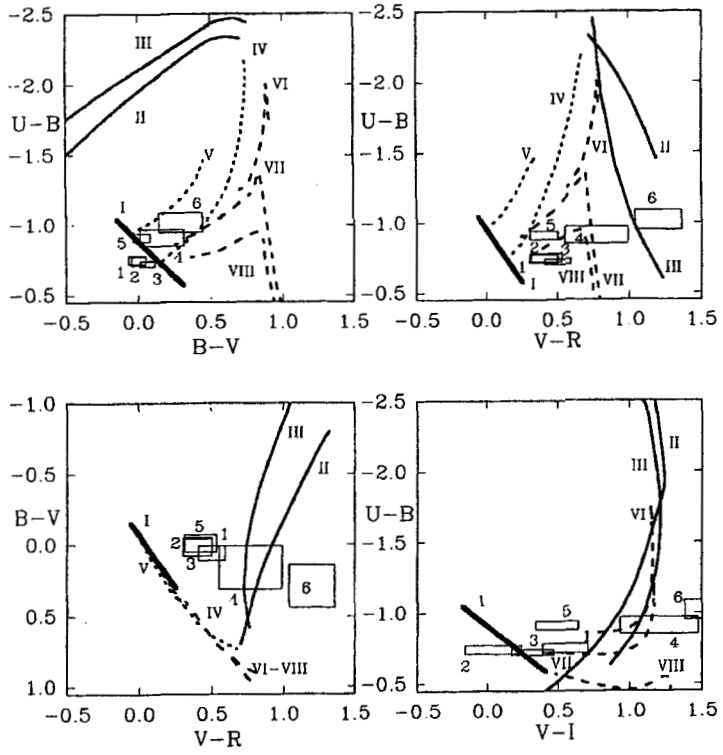

Figure 7 Colour–colour diagrams for pure flare radiations of two strong flares of EV Lac and several theoretical models of emission mechanisms: I, *black body* radiation for temperatures within the range from 6000 up to 20000 K; II and III, radiation of *hydrogen plasma optically thin in the Balmer continuum (Ba_C)* at an electronic temperature 10000 K and electron densities of 10^{12} and 10^{14} cm^{-3}; IV and V, radiation of *hydrogen plasma optically thick in Ba_C* at electron temperatures of 10000 and 15000 K, respectively; VI, VII and VIII, radiation of the *layers of the atmosphere of a dwarf star, heated by a flux of fast particles.* The numbering of rectangles corresponds to the vertical lines in Figure 6.

radiation from *black body* toward *hydrogen plasma* or *layers of stellar atmosphere heated up by fast particles* in the $(U-B, B-V)$ and the $(U-B, V-R)$ diagrams. In the $(B-V, V-R)$ diagram we see the location of flare radiation within the area of *hydrogen plasma* for the flare on 31.8.94 and a shift out of bound of the location of the considered sources for the flare 3.9.95. For both these flares in the $(U-B, V-I)$ diagram we find the location of flare radiation within the area of *hydrogen plasma* or *layers of stellar atmosphere heated up by fast particles* or a shift out of bound of the location of the discussed sources.

Thus, the colourimetric analysis of the observations of powerful flares of EV Lac in 1994 and 1995 confirms our previous conclusion: at any stage of development of such flares no single radiation mechanism among those concerned – *black body, optically thin and thick (in the Balmer continuum) hydrogen plasma and layers of*

stellar atmosphere heated by fast particles – can explain the observable properties of flare radiation within the whole *UBVRI* range of wavelengths. A full explanation would require some combination of the considered radiation mechanisms, for example, a short-lived *black body* radiation plus a *hydrogen plasma emission* of some optical thickness, or the development of a more sophisticated non-uniform model of stellar flares.

2.3 Spottedness of EV Lac in 1994–95

The photometric monitoring for EV Lac in the Crimea was interrupted every 30–40 min for *UBVRI* measurements of the comparison star SAO 52337. Thus, the data obtained permit us to study both the flare activity of the star, considered above, as well as the slow brightness changes of small amplitudes, which are due to heterogeneities of the star's spottedness.

The nightly averaged brightness of EV Lac is shown in Figure 8. The drawing shows slow variations with an amplitude $\Delta V = 0.02$ mag in 1994 and $\Delta V = 0.04$ mag in 1995.

Using a similar procedure of analysis as in previous campaigns, we evaluated the differential spottedness between bright and dark hemispheres of the star and the starspot temperature, using simple relations without accounting for the limb-darkening effect (Gershberg *et al.*, 1991b). Within the framework of such an approximation, the mentioned brightness amplitudes correspond to differential spottedness of the EV Lac hemispheres of 3.9% in 1994 and of 7.7% in 1995, and to a temperature difference between the quiet photosphere and the starspot regions of 240 and 250 K.

Recently Alekseev and Gershberg (1996a–c) have offered and developed a model of zonal spottedness for red dwarfs. In this model one takes into account both the effect of limb-darkening and absolute maximum of the stellar brightness, found from long-term photometric measurements. Applying this model to our observations, we found the following estimations concerning the absolute spottedness of the star: in 1994 the brightest hemisphere was covered by starspots up to 6.3%, and the darkest hemisphere by 7.5%; in 1995 the corresponding values were 8.9% and 11.0% respectively; the starspot temperature was lower by 210–220 K compared to the quiet photosphere.

In 1995 from June 27 to September 4 independent observations of the EV Lac spottedness were carried out by S. V. Pustil'nik, G. Sh. Roizman and G. P. Sigal at the Sea of Galilee Astrophysical Observatory, Israel. Observations were carried out at the 16-inch Schmidt–Cassegrain telescope with the ST-6 CCD camera for *BVR* photometry. The primary reduction was fulfilled by an aperture photometry with elliptical digital diaphragms which were chosen using an isophot system. The data obtained in the *V*-band are given in the lower panel of Figure 8. They contain an order of magnitude more measurements than the Crimean data, and independent processing of these observations within the framework of the zonal model of stellar spottedness gave much better results. However, spottedness parameters obtained from these data – 9.2% and 11.5% of the stellar surface occupied by starspots and

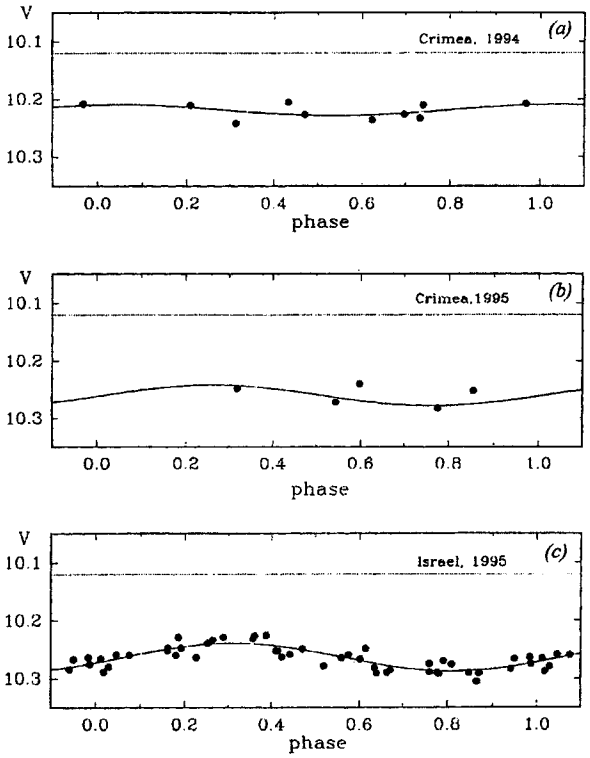

Figure 8 Nightly averaged magnitudes of EV Lac in the quiet state in 1994 (*a*) and in 1995 (*b*), measured in Crimea, and measured in 1995 (*c*) at the Sea of Galilee Astrophysical Observatory, Israel. The absolute maximum of the stellar brightness is indicated by the dashed line.

the temperature difference for the quiet photosphere and starspots of 210 K – turned out to be very close to those determined from the Crimean observations.

3 SPECTRAL OBSERVATIONS

Spectral monitoring of EV Lac was carried out in 1994 and in 1995 with the Shajn 2.6 m reflector of the Crimean Astrophysical Observatory by S. V. Berdyugina, R. E. Gershberg, N. I. Shakhovskaya and V. A. Shcherbakov.

3.1 Results of Observations in 1994

In 1994 spectral observations of EV Lac were carried out in the region of the H_β line with the technique described in detail earlier (Abdul-Aziz *et al.*, 1995). The SPEM spectrograph installed at the Nasmyth focus supplied with the Russian CCD system

Table 4. Characteristics of the EV Lac spectra in the quiet state in 1994

Nights	*26.8*	*27.8*	*28.8*	*29.8*	*30.8*	*31.8*
			Nightly averaged			
Summary exposure (min)	45	45	40	185	111	73
Number of spectra	3	4	4	18	11	7
W_β (Å)	4.9±0.1	4.8±0.1	5.0±0.1	4.7±0.1	4.4±0.1	5.0±0.2
FWHM$_\beta$ (Å)	4.6±0.1	5.0±0.1	4.9±0.1	4.6±0.1	4.9±0.1	3.7±0.1
FWQM$_\beta$ (Å)	6.2±0.03	6.7±0.02	7.1±0.1	6.7±0.1	6.9±0.1	5.8±0.1
W_γ (Å)	10.0±0.4	12.5±1.2	8.6±0.6	10.5±0.3	10.7±0.3	8.6±0.4
FWHM$_\gamma$ (Å)	4.5±0.2	5.4±0.3	5.9±0.1	5.7±0.1	5.5±0.2	4.7±0.2
FWQM$_\gamma$ (Å)	8.1±0.2	8.6±0.4	9.4±0.5	9.1±0.2	8.9±0.3	7.0±0.1
J 4761 Å	1.53±0.02	1.51±0.03	1.54±0.01	1.54±0.01	1.52±0.01	1.55±0.07
J 4955 Å	1.95±0.01	1.95±0.02	1.92±0.02	1.92±0.01	1.92±0.02	1.94±0.01
J 5448 Å			1.70±0.01	1.71±0.01	1.71±0.01	1.70±0.01
Phase of axial rotation period	0.30	0.50	0.75	0.98	0.22	0.43

Astro-550 ISTA was used; the CCD system contained 600×520 pixels (Berezin *et al.*, 1991). The diffraction grating with 600 grooves/mm provided a dispersion of about 100 Å/mm or 2.2 Å/pixel. The FWHM of the instumental profile was 4 Å for an entrance slit width of 1.″5. The grating was fixed for monitoring in the wavelength range from 4190 Å up to 5480 Å. Due to expansion of the registered range toward shorter wavelengths by 260 Å, as compared to the observations in 1992, spectra obtained in 1994 can be used to investigate the behaviour of two Balmer lines – H_β and H_γ – simultaneously. In the quiet state of the star the signal/noise ratio reached 140 in the centre of the H_β line, 90 in the adjacent continuum, 70 in the centre of the H_γ line and 30 in the adjacent continuum for exposures of 10 minutes. On both sides of the stellar spectrum the standard Ne–Ar lamp comparison spectrum was placed. The dead time between exposures in order to make a comparison spectrum and flat field and for the reading of the CCD was 1–2 minutes.

A total, 179 EV Lac spectra were recorded during this campaign. The majority was obtained with exposures of 10 minutes. Between observers at the Shajn reflector and AZT-11 a telephone link was maintained during the observations. Thus during the quiet state of the star, exposures were sometimes increased up to 15 minutes, whereas during flares they were decreased to 5 minutes.

3.1.1 Spectra of the quiet state of the star

By inspecting the U-band light curves of EV Lac and the temporal distribution of the obtained spectra we were able to select spectra which most probably corresponded to the undisturbed state of the star for each of the six nights. The quantitative characteristics of the night-averaged quiet state spectra and their root-

mean-square errors are listed in Table 4. The table shows that photospheric characteristics of the spectrum – the magnitudes of intensity jumps at the heads of TiO molecular bands $\lambda\lambda$ 4761 Å, 4955 Å and 5448 Å – were practically constant during the whole campaign and rather close to the values measured in 1992 (Abdul-Aziz *et al.*, 1995). Chromospheric characteristics – the equivalent widths of the emission lines H_β and H_γ and their full widths at levels of half and of quarter maximum intensity, – FWHM and FWQM, respectively – show rather small changes from night to night, which in several cases fall outside the limits of probable errors of measurements. Since the values of FWHM are determined mainly by instrumental profiles, their variations from night to night are less noticeable than changes of equivalent widths of lines. But considering variations of equivalent widths it is possible to find some repeatability of appropriate values through four days, the period of axial rotation of the star; this fact can be connected to the non-uniformity of the stellar chromosphere and regarded as a proof of the reality of such changes. The phases of the stellar axial rotation period of the star are given in the last line of Table 4. Finally, the closeness of the FWHM of H_β in 1992 and 1994 should be noted, while equivalent widths of this line in 1994 were significantly larger than in 1992.

3.1.2 Spectra of the active state of the star

An increase of the stellar brightness by $\Delta U \sim 0.10$–0.15 mag or more is accompanied, as a rule, by changes of chromospheric spectrum characteristics. However, for a quantitative discussion of such changes, only long-lasting flares are suitable, for which our 5–10 minute spectral exposures do not blend with the quiet state of the star.

The H_β and H_γ emission lines

In Figure 9 the U-band light curves together with all equivalent widths of the emission lines H_β and H_γ are gathered for four nights, when flares of noticeable amplitudes were observed; the 2σ error values of measurements indicated in the plots were determined from the scatter of the corresponding measurements in the quiet state of the star for each night. The plots show a close correlation between W_{H_β} and W_{H_γ}, while a connection between these values and the brightness of the star in the U-band is not so clear. The absence of a strict linear dependence between the equivalent widths of the two Balmer lines is apparently due to the finite optical thickness of the matter of flares in these lines and, possibly, to various contributions of flare emission to the adjecent continuum. Concerning the slower fading of flares in lines compared to the fading rate in the U-band, this fact was already found during the first simultaneous photometric and spectral observations of stellar flares with high temporal resolution (Gershberg and Chugainov, 1966, 1967; Kunkel, 1970; Bopp and Moffett, 1973; Moffett and Bopp, 1976), and our results confirm earlier conclusions obtained with photographic techniques.

As is known, the main difference between the profiles of emission lines in the UV Cet-type flare star spectra taken during flares and in the quiet state of the

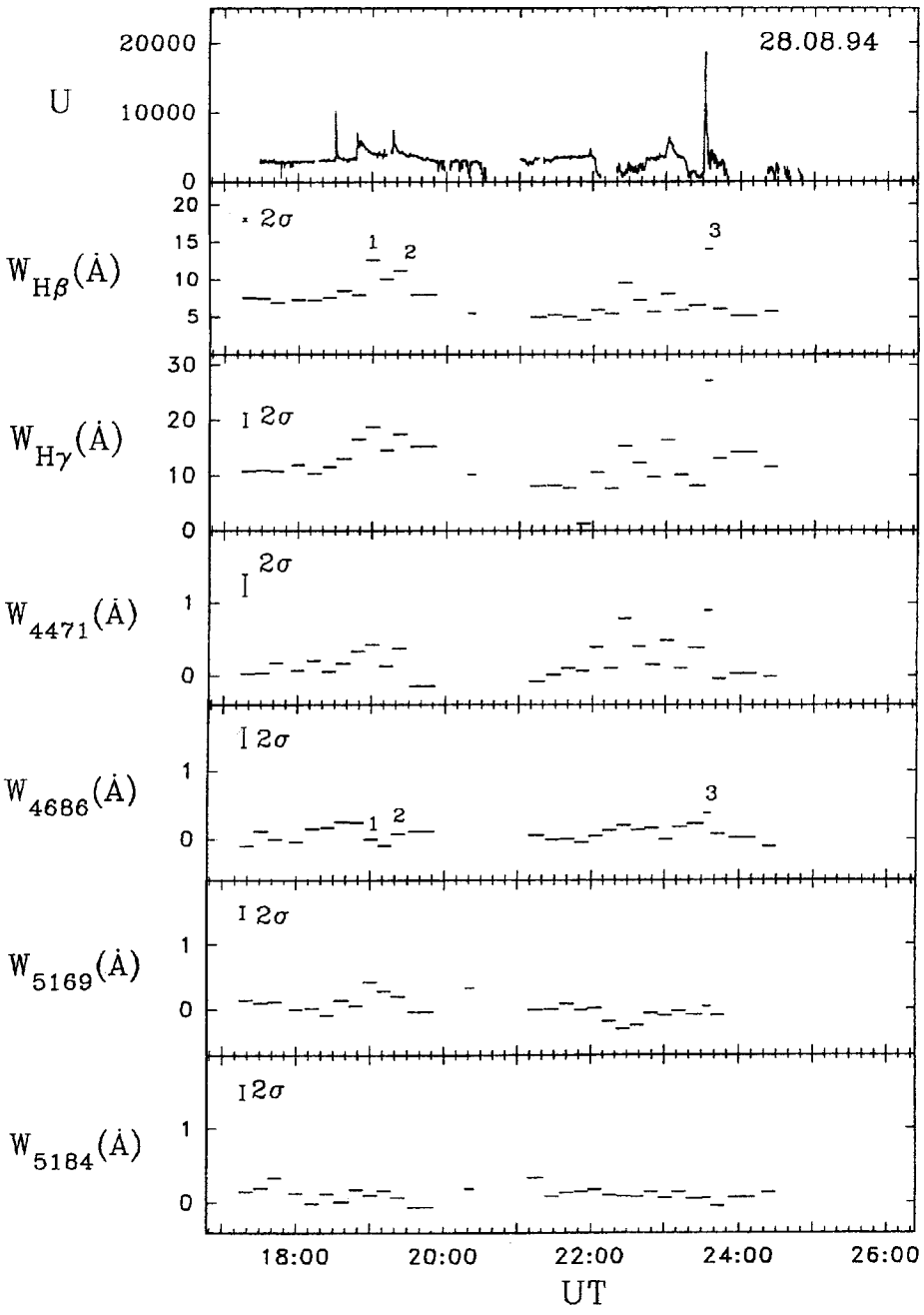

Figure 9 The *U*-band light curves of EV Lac and simultaneous measurements of the equivalent widths of the emission lines H_β, H_γ, He I λ 4471 Å, He II λ 4686 Å, blend λ 5167–73Å and line Mg I λ 5184 Å.

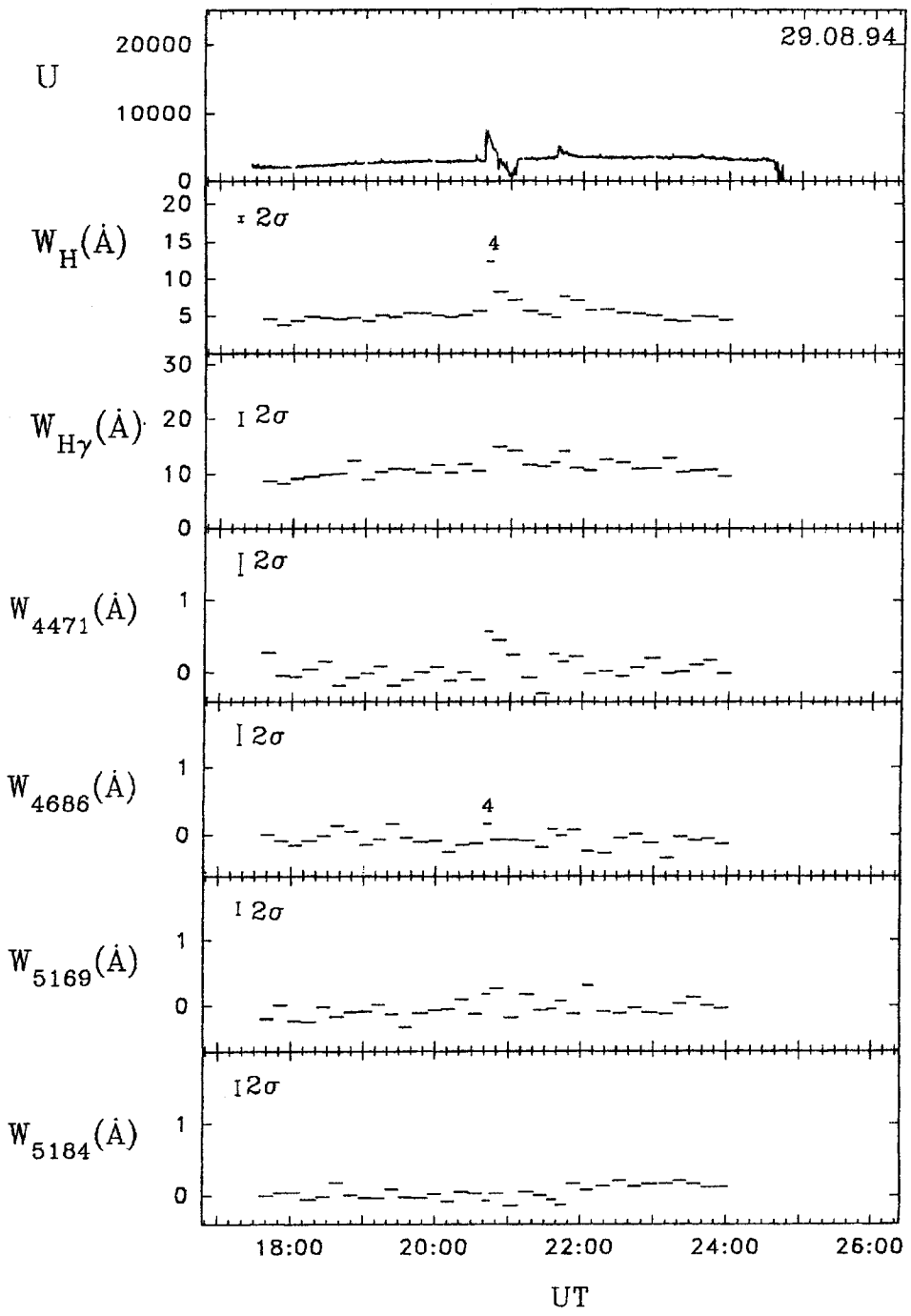

Figure 9 Continued.

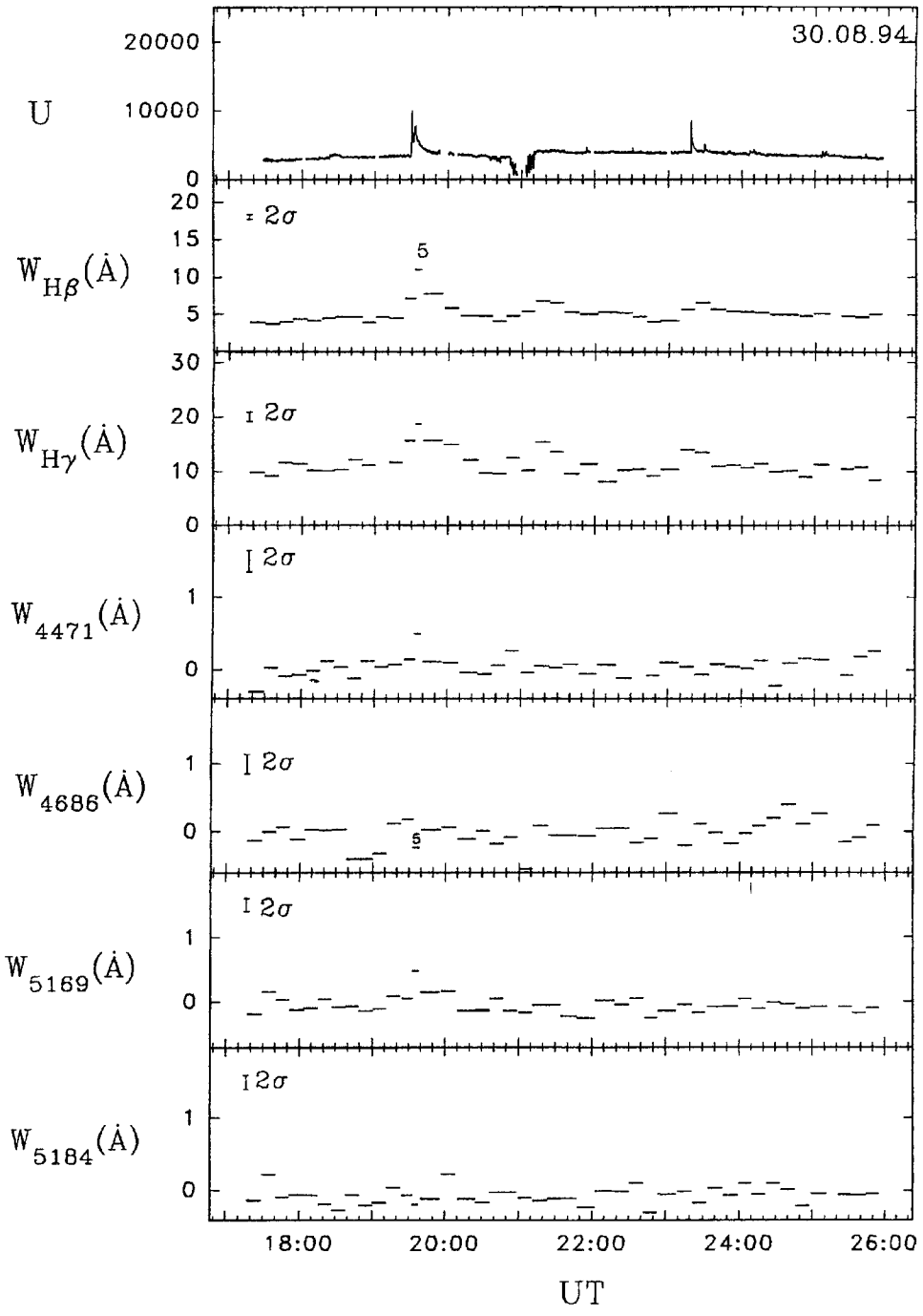

Figure 9 Continued.

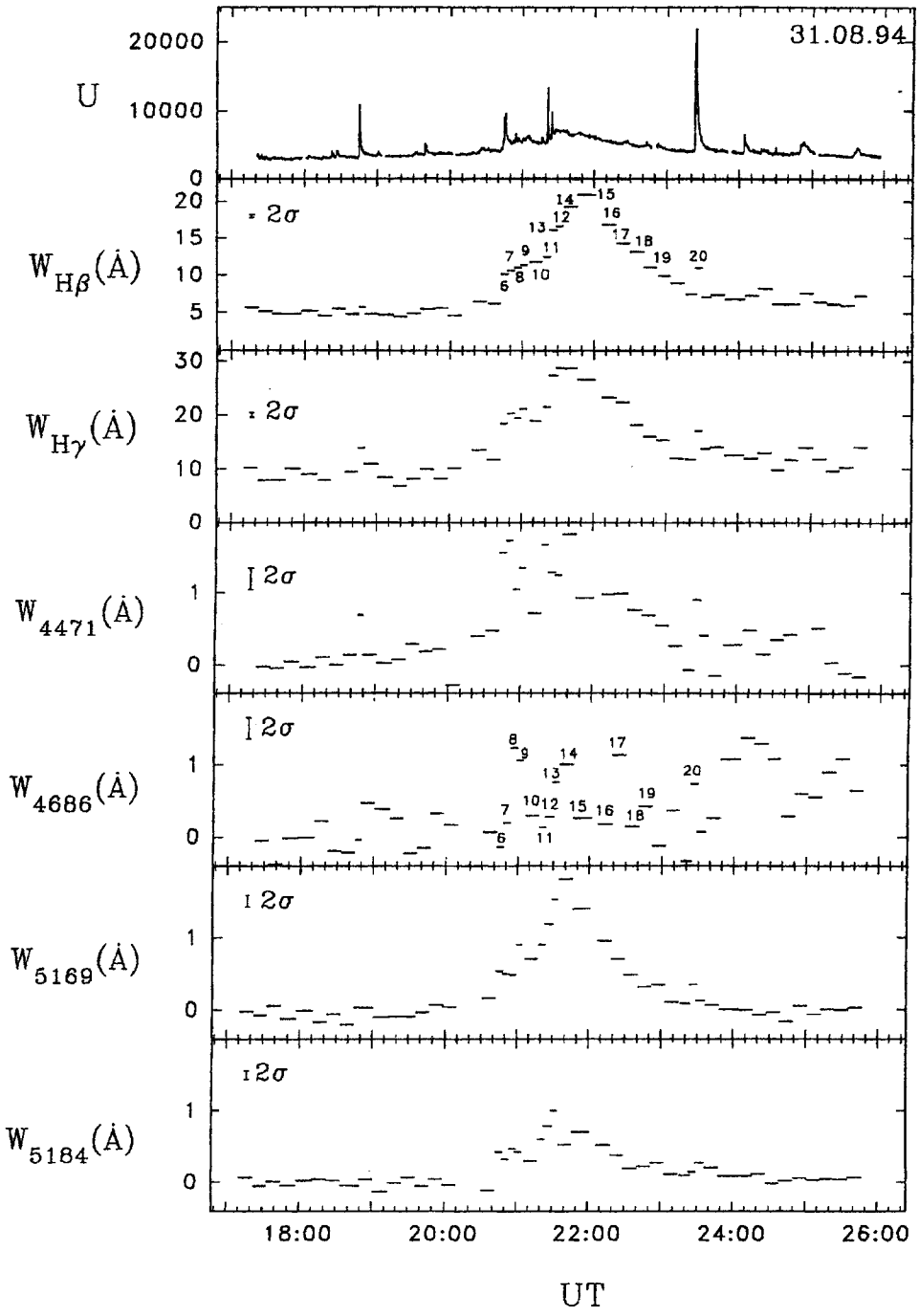

Figure 9 Continued.

star is the appearance of wide wings, frequently asymmetric, during flares. For the quantitative consideration of the EV Lac emission lines' profiles obtained by us during the active state of the star, we have selected all spectrograms with appreciably increased equivalent widths of the H_β line or with noticeable broadening of this line at the level of 1/4 of maximum intensity (FWQM). The twenty selected spectra are numbered in Figure 9 and their quantitative characteristics – equivalent widths of the emission lines H_β and H_γ and total widths of these lines at the level of 1/4 maximum intensity (FWQM) – are presented in columns 4 to 7 of Table 5. In the last line of the table correlation coefficients between the H_β and H_γ line parameters are given. The first five of the selected spectra refer to rather short flares on 28.8.94 at UT 18:48, 19:17, 23:32, on 29.8.94 at UT 20:39 and to the flare on 30.8.94 at UT 19:30 with two maxima. The other 15 spectra cover a 3-hour interval of the active state of the star on 31.8.94 at UT 20:30–23:30, during which at least eight fast flares of various amplitudes and the slow fading of the stellar brightness after the double flare at UT 21:21 took place. To all these spectra the technique of picking out an active state spectrum described earlier (Abdul-Aziz *et al.*, 1995) was applied for every active state spectrum: the average quiet state spectrum taken during the same night was subtructed by the following procedure

$$\begin{aligned}[\text{pure spectrum of flare}] &= [\text{record of spectrum of a flare}] \\ &- \kappa[\text{record of a quite spectrum for the same night}] \quad (1)\end{aligned}$$

The factor κ was fitted to minimize the intensity jump at the head of the TiO molecular band λ 4955 Å in the pure spectrum of the flare. The widest eight of the obtained profiles are shown in Figure 10: thick solid lines relate to H_β, thin solid lines to H_γ, the values of their $FWHM_{fl}$ and $FWQM_{fl}$ are given in columns 8–11 of Table 5.

The 20 selected profiles of the pure flare spectra were then presented as sums of Gaussian components.

Firstly, following Doyle and Byrne (1987), every profile was represented by a sum of two Gaussians and their widths, intensities and central wavelengths were fitted to the observed profiles. The results are given in columns 12–17 of Table 5. The table shows that practically all of the considered profiles can be represented by a sum of two rather desimilar Gaussians: a narrow component with high intensity at the centre and a wide component with low central intensity. The $FWHM_{nar}$ of the narrow components – see columns 12 and 13 – is very close to the widths of the instrumental profiles, and the $FWHM_{wid}$ of the wide components – see columns 14 and 15 – a few times larger and exceeds 20 Å for the 15th and 20th spectra, which were obtained during the maximum of W_{H_β} on 31.8.94, close to UT 22:00 and during the fast flare of large amplitude on 31.8.94, UT 23:24 respectively. During fast flares, the wide components contribute appreciably or even mostly to the total emission in the considered lines – see columns 16 and 17 of Table 5 – but their share drops to negligible values during the smooth fading of the emission in the slow event on 31.8.94. In Figure 10 the observed profiles of the H_β line, represented by a sum of two Gaussians, are given by dashed lines. The relative shifts of the centres of the

Table 5. Characteristics of the EV Lac spectra in the active states in 1994

NN	*Date and UT of beginning and end of exposure*					*Amplitudes* $\Delta U(mag)$ *beginning*	*end*	*averaged*	W_λ β	W_λ γ	$FWQM$ β	$FWQM$ γ	$FWHM_{fl}$ β	$FWHM_{fl}$ γ	$FWQM_{fl}$ β	$FWQM_{fl}$ γ	$FWHM_{nar}$ β	$FWHM_{nar}$ γ	$FWHM_{wid}$ β	$FWHM_{wid}$ γ	E_{wid}/E_{tot} β	E_{wid}/E_{tot} γ
1	28.8	22^h	21^m	51^s-32^m	01^s	no photometry			12.6	18.7	7.3	9.2	3.7	5.4	6.1	7.3	3.8	4.1	12.2	11.4	0.25	0.33
2		23	31	58 – 37	08	no photometry			11.1	17.4	7.3	8.6	3.8	4.8	5.8	6.4	3.6	3.8	16.0	11.4	0.19	0.29
3	29.8	20	39	38 – 45	10	0.70	0.56	0.80	14.0		9.8	15.1	6.5	8.1	11.6	16.2	4.6	4.8	15.7	18.0	0.59	0.74
4	30.8	19	25	07 – 33	15	0.00	0.76	0.33	12.4	23.4	8.4	12.8	6.0	7.8	11.5	16.9	3.6	4.8	13.8	19.5	0.73	0.70
5		19	33	25 – 38	15	0.82	0.34	0.54	11.0	18.8	7.4	9.7	4.9	6.2	8.2	10.0	3.8	5.4	11.0	17.0	0.50	0.37
6	31.8	20	43	06 – 48	19	0.17	0.47	0.58	10.2	18.6	7.6	9.7	4.4	6.9	10.1	11.0	3.6	4.0	16.0	11.6	0.64	0.49
7		20	48	30 – 53	19	0.44	0.39	0.40	10.6	20.4	7.4	10.2	5.3	6.3	9.8	10.0	3.6	5.7	12.6	21.7	0.65	0.32
8		20	54	10 – 59	19	0.50	0.38	0.47	11.0	19.5	7.2	8.6	5.7	5.6	9.0	9.1	4.1	4.2	11.0	12.1	0.47	0.52
9		20	59	20 – 04	19	0.41	0.53	0.46	11.4	21.2	7.5	9.3	5.3	5.2	8.5	9.0	3.6	3.8	9.6	8.8	0.54	0.53
10		21	07	19 – 17	19	0.50	0.45	0.39	11.8	19.0	6.8	7.5	4.0	5.2	7.2	7.2	3.6	3.8	11.0	8.4	0.37	0.38
11		21	18	10 – 24	17	0.39	0.47	0.52	12.5	21.5	7.0	8.5	4.0	5.9	7.3	8.8	3.6	3.8	12.0	8.1	0.39	0.56
12		21	24	27 – 29	17	0.60	0.66	0.68	16.1	27.4	6.9	8.3	4.0	5.6	7.2	8.3	3.6	3.8	12.7	9.4	0.36	0.23
13		21	29	27 – 34	17	0.64	0.65	0.65	16.6	28.9	6.5	6.7	4.0	4.5	6.3	6.6	3.6	3.8	14.4	7.2	0.27	0.23
14		21	35	44 – 45	55	0.63	0.57	0.58	19.3	28.8	6.4	7.5	3.6	5.1	6.2	7.0	3.6	3.8	14.7	6.2	0.19	0.24
15		21	46	47 – 01	08	0.62	0.58	0.43	20.9	26.6	6.2	6.7	3.5	4.5	5.7	6.4	3.6	3.8	25.0	7.0	0.16	0.21
16		22	07	34 – 18	18	0.37	0.33	0.37	16.8	23.3	6.0	7.3	4.3	4.3	5.9	6.6	3.6	3.8		8.8		0.18
17		22	19	11 – 29	27	0.29	0.30	0.33	14.3	22.3	6.3	7.5	3.7	5.0	5.8	6.6	3.6	4.1	14.6	30.4	0.12	0.21
18		22	30	21 – 40	34	0.28	0.21	0.23	13.1	18.2	6.2	7.4	4.3	3.7	6.0	6.2	3.6	3.8	6.3	12.1	0.06	0.12
19		22	41	31 – 51	39	0.23	0.18	0.23	11.1	16.0	6.0	7.7	3.5	3.5	5.5	6.2	3.6	3.8	8.1	9.4	0.04	0.14
20		23	16	19 – 24	09	0.02	1.80	0.50	11.0	17.2	7.1	11.1	3.6	5.8	7.1	12.1	3.6	3.8	21.4	13.3	0.49	0.68
r									0.84		0.93		0.70		0.90		0.39		−0.01		0.80	

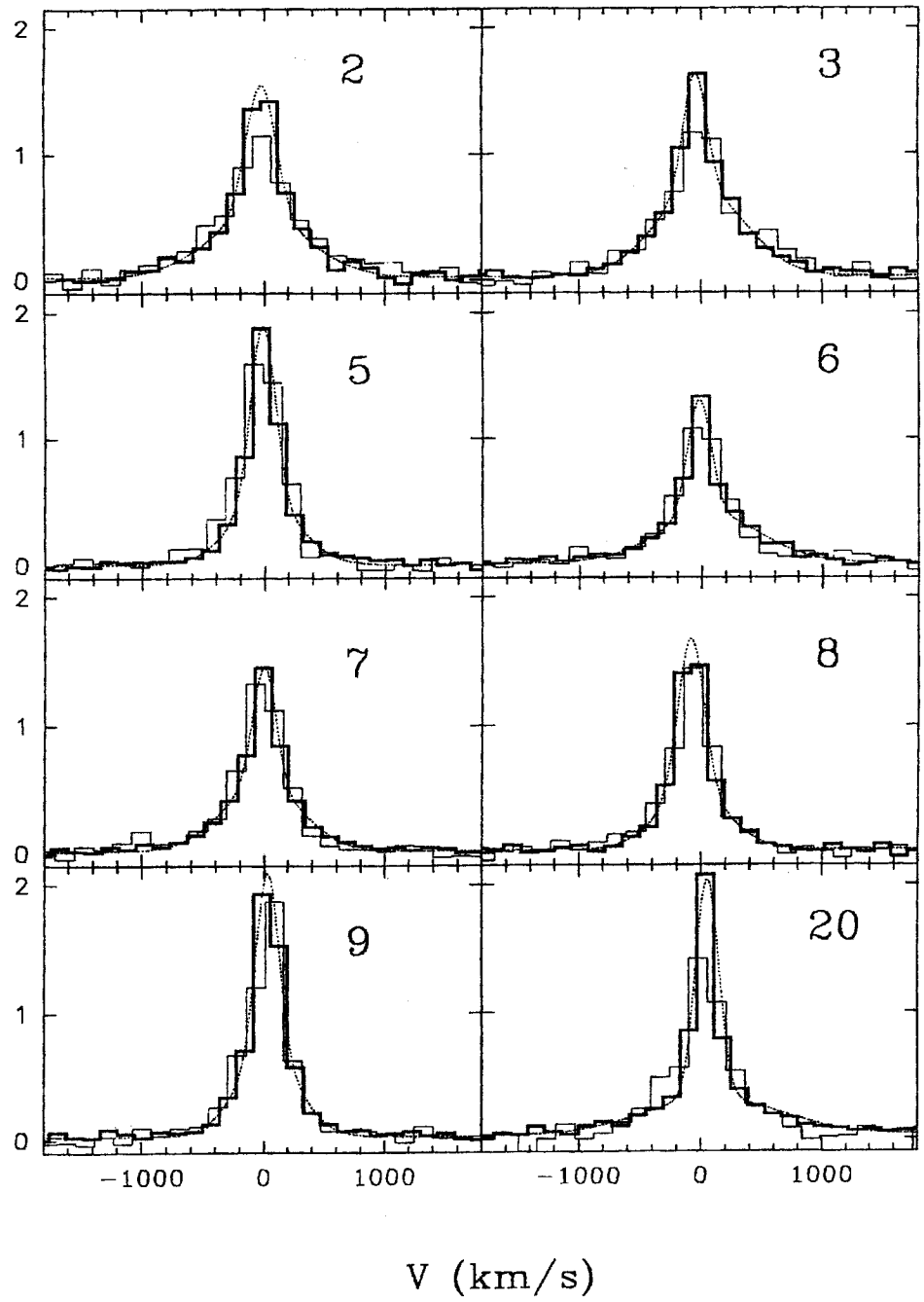

Figure 10 Profiles of emission lines: H_β – thick solid lines – and H_γ – thin solid lines – in pure active state spectra and representation of H_β profiles with two Gaussians – dashed lines.

narrow and the wide components of both signs do not exceed, as a rule, 100 km/s, the pixel size in our velocity scale.

Then, as in the analysis of the 1992 observations (Abdul-Aziz *et al.*, 1995), the selected profiles of emission lines of pure flare spectra, were fitted by sums of several Gaussians with instrumental widths but with different central intensities and with various shifts along the velocity axis. In all cases five or less such components were enough for a good representation of the observations and root-mean-square velocities between the components turned out to be within the range between 400 and 700 km/s.

Emission lines of helium and metals

Analysing the 1992 spectral observations, we have coadded all pure flare spectra and identified 10 lines of He, Fe and Mg in the composite spectrum – see Figure 15 in Abdul-Aziz *et al.* (1995). In the course of this identification we used earlier spectral observations of flares of the UV Cet-type stars (Joy and Humason, 1949; Gershberg and Chugainov, 1966, 1967; Greenstein and Arp, 1969; Bopp and Moffett, 1973; Mochnacky and Shommer, 1979), observations of T Tau-type stars (Joy, 1945), solar flares (Severny *et al.*, 1960) and solar prominences (Tandberg-Hanssen, 1963).

A similar composite pure spectrum of flares, observed in 1994, is given in Figure 11. All non-hydrogen lines detected in 1992 are easily seen in this plot. In addition, a cross-examination of the 1992 and the 1994 composite spectra permitted the identification in both spectra of the following additional lines: the He I λ 4713 Å line, which was suggested by Greenstein and Arp (1969) in the spectrum of the Wolf 359 flare, the Fe I (36) λ 5042 Å line, detected earlier in solar flares (Severny *et al.*, 1960), and the Ti I (4) λ 5210 Å line.

Among several detected lines of neutral helium the λ 4471 Å line is the strongest. Monitoring of the temporal variations of the intensity of this line during the prolonged activity of the star on 31.8.94 shows that it responds faster to the beginning of fast flares in the U-band. But it is not clear whether this feature is similar to the fast bursts of the He I λ 4922 Å, detected by Bopp and Moffett (1973) in the flare on UV Cet on 14.10.72 at UT 08:29. All our measurements of equivalent widths of the He I λ 4471 Å line are presented in the fourth panel in Figure 9. During the 31.8.94 observation the correlation coefficient between these values and W_{H_β} was $r(W_{4471}, W_{H_\beta}) = 0.76$.

In Figure 11 the split of the He II λ 4686 Å attracts attention: the component shifted by –400 km/s is no less intense than the non-shifted one. The consideration of individual spectra, numbered in Figure 9, has revealed that this splitting effect in the composite spectrum is caused by spectra, taken on 31.8.94 – NN 9, 13, 14, 17 and 19 – which, as already noted, cover a number of fast flares and subsequent slow brightness fading of the star. Only blue-shifted He II emission is seen in three consecutive spectra, obtained on 31.8.94 after the strong flare at UT 23:24 in the time interval UT 23:49–24:27, including the fast flare with the brightest maximum at UT 24:04 – see Figure 9. A careful examination of the composite pure spectrum of flares of EV Lac in 1992 permits us to suggest some strengthening of the blue

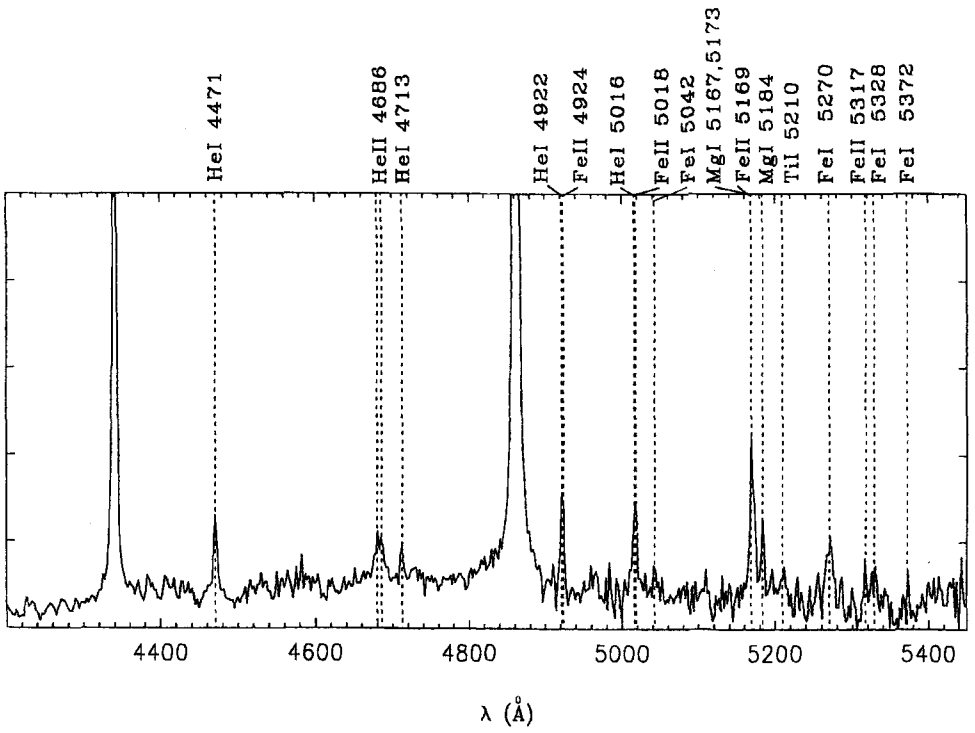

Figure 11 Composite pure flare spectrum for events listed in Table 5.

wing of this He II line. All measured values of W_{4686} are presented on the fifth panel in Figure 9. (For convenience of consideration in this fifth panel the numbering of pure spectra chosen for analysis of flares is repeated.) It should be noted that the He II $\lambda\lambda$ 4686 Å line is rather rarely detected in flares of the UV Cet-type stars and so the prolonged emission in this line on the 31.8.94 spectrum of EV Lac can be thought of as an exclusive event. It is possible that the long-lived emission of He II λ 4686 Å in the EV Lac spectrum has the same physical nature as the long enhancement of the He II λ 1640 Å in the AD Leo spectrum after the impulsive flare observed on 2.2.83 (Byrne and Gary, 1989).

Finally, the data on emission lines of metals in the EV Lac spectra are presented in the two bottom panels in Figure 9.

In the sixth panel the measurements of the blend, which includes two components of the Mg I (2) triplet, the component of the Fe II (42) triplet and two weaker lines from the Fe I (36) and (37) multiplets, are given. Apparently, the main contributor to this blend is the Fe II (42) λ 5169 Å line. Indeed, the two Mg I (2) components, involved in this blend, should be close in sum to the separately registered λ 5184 Å component (Joy, 1945), but this component, as Figure 11 shows, is much weaker than the considered blend. The correlation coefficient between the

equivalent widths of the blend and H_β throughout the night of 31.8.94 is rather high: $r(W_{5169}, W_{H_\beta}) = 0.94$, which permits us to believe that emissions of hydrogen and the considered triplet of Fe II are located at the same layer within the flares.

In the seventh panel in Figure 9 the equivalent widths of the strongest component of the Mg I (2) triplet λ 5184 Å are presented. The drawing shows that variations of this emission correlate well with the majority of the previously considered emissions: $r(W_{5184}, W_{H_\beta}) = 0.89$, $r(W_{5184}, W_{5169}) = 0.91$ and $r(W_{5184}, W_{4471}) = 0.77$. The rather weak lines of Fe I (15, 37) λ 5270 Å and Ti (4) λ 5210 Å correlate with the mentioned emission as well: $r(W_{5270}, W_{H_\beta}) = 0.91$, $r(W_{5270}, W_{5169}) = 0.86$, $r(W_{5270}, W_{5184}) = 0.87$, $r(W_{5270}, W_{4471}) = 0.68$, $r(W_{5270}, W_{5210}) = 0.85$, $r(W_{5210}, W_{H_\beta}) = 0.77$, $r(W_{5210}, W_{5169}) = 0.78$, $r(W_{5210}, W_{5184}) = 0.89$ and $r(W_{5210}, W_{4471}) = 0.68$. The above analysis shows that there is a better correlation of the H_β intensities with metals, than with the He I λ 4471Å line. From this general regularity the He II λ 4686 Å drops out obviously: the correlation coefficients between this line and the other considered ones are within the range from 0.20 to 0.33. This suggests that the regions of formation of He II and the other detected emissions are located in different layers of the excited atmosphere of the star.

Continuum emission of flares

The intensity of continuum emission of a flare can be evaluated by exact measurements of the veiling of intensity jumps at the heads of TiO molecular bands (Abdul-Aziz *et al.*, 1995). Indeed, if the magnitude of an intensity jump $J = I_{\lambda-}/I_{\lambda+}$ is J_q in the quiet state of the star and J_f during a flare, then the intensity of the continuum emission of the flare ΔI near the jump is defined by the relation

$$\Delta I/I_{\lambda-} = (J_q - J_f)/J_q(J_f - 1). \tag{2}$$

This relation can give confident results only if the accuracy of measurements of J_q and J_f is high enough. The accuracy of measurements δJ_q is given in Table 4; the accuracy of measurements δJ_f during flares can be evaluated as

$$\delta J_f = \left(\frac{\Sigma t_q}{t_f}\right)^{1/2} \times \delta J_q, \tag{3}$$

where Σt_q is the sum of exposure times of the star in the quiet state during the relevant night, listed in Table 4, and t_f is the exposure time of the spectrum taken during the flare. Using these values δJ_q and δJ_f, we have found that from all spectra, listed in Table 5, only in three cases do the ratios $\Delta I/I_{\lambda-}$ exceed by several times the corresponding errors of their determination: the measured intensity jump at λ 4955 Å turned out to be equal to 0.17 ± 0.05, 0.09 ± 0.03 and $0.08 + 0.02$ in the spectra NN 3,4 and 14. The intensity jump at λ 4955 Å lies close to the middle between the effective wavelengths of the B and the V bands. Therefore, the veiling of this jump should correlate with the amplitude of a flare: $\Delta m = (\Delta B + \Delta V)/2$. Unfortunately, only for the spectrum N 14 among the three considered jumps do

we have enough reliable photometric measurements: $\Delta m = 0.13$ mag; as far as $1 - \mathrm{dex}(-0.4 \times 0.13) = 0.11$, concerned spectral and photometric measurements give rather well agreeed estimations of the flare continuum.

3.2 Results of Observations in 1995

In 1995 the spectral observations of EV Lac at the Shajn 2.6 m telescope were carried out in the region of the H_α line with the coude spectrograph supplied with the CCD system Photometrics Ltd SDS–9000. The CCD's length is 28 mm and has 1024 × 256 pixels. The diffraction grating with 600 grooves/mm was installed to work in the second order for the first night of observations and in the first order for the other four nights. In the second order the grating gave a dispersion of 2.4 Å/mm (or 0.065 Å/pixel) and a spectral resolution of 0.37 Å for an entrance slit of 1.″0; the wavelength range between 6530 Å and 6598 Å was covered. In the first order the grating gave a dispersion of 4.8 Å/mm (or 0.13 Å/pixel), spectral resolution 0.74 Å for the same slit and the wavelength range from 6500 Å to 6632 Å was covered. The dead time interval between consequent exposures needed to make a comparison spectrum, flat field and to read the CCD was 1–2 minutes.

As in 1994, between observers at the Shajn reflector and AZT-11 a phone link was maintained, and during the quiet state of the star exposures were increased up to 30 minutes, while during flares they were decreased to 5–10 minutes. In the quiet state of the star the signal/noise ratio reached 150 in the centre of the H_α line and 90 in the adjacent continuum.

In total 64 spectra of EV Lac were registered during this campaign.

3.2.1 Spectra of the quiet state of the star

Using the U-band light curves of EV Lac for each night, we selected spectra which corresponded to the quiet state of the star with a high probability, that is free from flare effects. The nightly averaged quantitative characteristics obtained from these spectra and their probable errors are given in Table 6. One spectrum of 1.9.95, when

Table 6. Characteristics of the EV Lac spectra in the quiet state in 1995

Nights	*31.8*	*1.9*	*2.9*	*3.9*	*4.9*
			Nightly averaged		
Number of spectra	4	1	6	8	4
Summary exposure (min)	104	15	180	240	114
W_{H_α} (Å)	5.35±.24	4.00	3.52±.04	3.80±.04	4.70±.16
FWHM_{H_α} (Å)	1.31±.04	1.34	1.37±.01	1.36±.01	1.39±.01
FWQM_{H_α} (Å)	1.59±.01	1.79	1.78±.01	1.78±.01	1.80±.02
$W_{CaI\ \lambda 6573}$ (Å)	0.58±.02	0.45	0.50±.01	0.51±.01	0.48±.01
Phase of axial rotation period	0.02	0.22	0.50	0.71	0.96

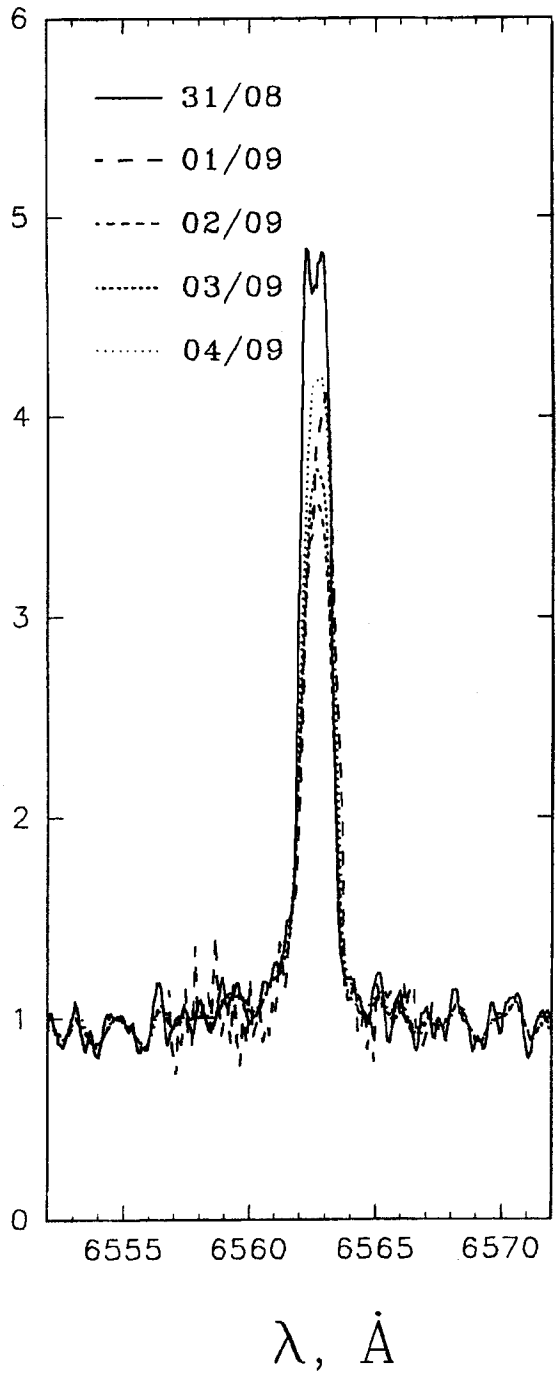

Figure 12 Nightly averaged H_α profiles for the quiet state of the star in 1995.

the weather conditions did not allow us to carry out the photometric patrol, is also included in Table 6. For each night, Table 6 gives the values of equivalent widths of the H_α line, its total widths at levels of half and quarter maximum intensities and the equivalent width of the strongest absorption line within the wavelength range considered – Ca I (1) λ 6573 Å. In the last line of Table 6 the phases of the axial rotation period, calculated for the brightness minima of the star, are given; these minima correspond to times when the most spotted region of the star passed through the central meridian – see Figure 8.

Both the average values of W_{H_α} and their variations from night to night are close to the corresponding values obtained during the EV Lac campaign in 1990 (Gershberg *et al.*, 1993).

In Figure 12 nightly averaged quiet state H_α line profiles corresponding to the four nights in Table 6 are shown. Every profile is normalized to the corresponding local continuum of the stellar spectrum. Therefore, the differences of the profiles visible in Figure 12 are caused by both different absolute intensities of the line and differences in the absolute levels of the local continuum, which are due to brightness variations, caused by the non-uniform spottedness of the rotating star. However, since the rotational modulation of the EV Lac brightness in the R-band does not exceed $0^m.04$, the variations of the absolute continuum levels in these nights cannot be more than 4%. Therefore the decisive factor in the variations of the intensity of the profiles in Figure 12 is the differences in the absolute intensities of the chromosphere on different longitudes of the star. Table 6 and Figure 12 show an appreciable excess of W_{H_α} values on dates 31.8 and 4.9 above these values in other nights. The closeness of phases of the axial rotation period of the star on these two nights suggests that the noted excess is caused by the passing of the same active area with powerful chromospheric emission through the visible disk of the star.

The H_α line recorded on 31.8.95 with the spectral resolution of 0.37 Å showed a two-peaked structure in the centre of the profile. During the subsequent nights, when twice the lower spectral resolution was used, this structure was not seen.

3.2.2 H_α *emission in the active state of the star*

In Figure 13 vertical positions of the horizontal lines indicate the values of the equivalent widths W_{H_α} and the U-band light curves are also shown. From this plot 14 spectra with the largest W_{H_α} were selected for further consideration. We consider these spectra to be connected with the active state of the star. On the drawing the selected spectra are numbered.

The drawing shows that there exists no unique relation between the W_{H_α} and the stellar brightness: several spectra with large W_{H_α} correspond to times of brightness maxima of flares (NN 1,3,5,8), others to fading phases of flares (NN 2, 4, 6), and the strongest emission of the H_α line took place during more than 3 hours after the rather short flare on 4.9.95 at about UT 18:00–18:10; this event reminds us of the prolonged enhancement of emission lines in the green region of the EV Lac spectrum on 31.8.94 at UT 20:30–23:20 described above.

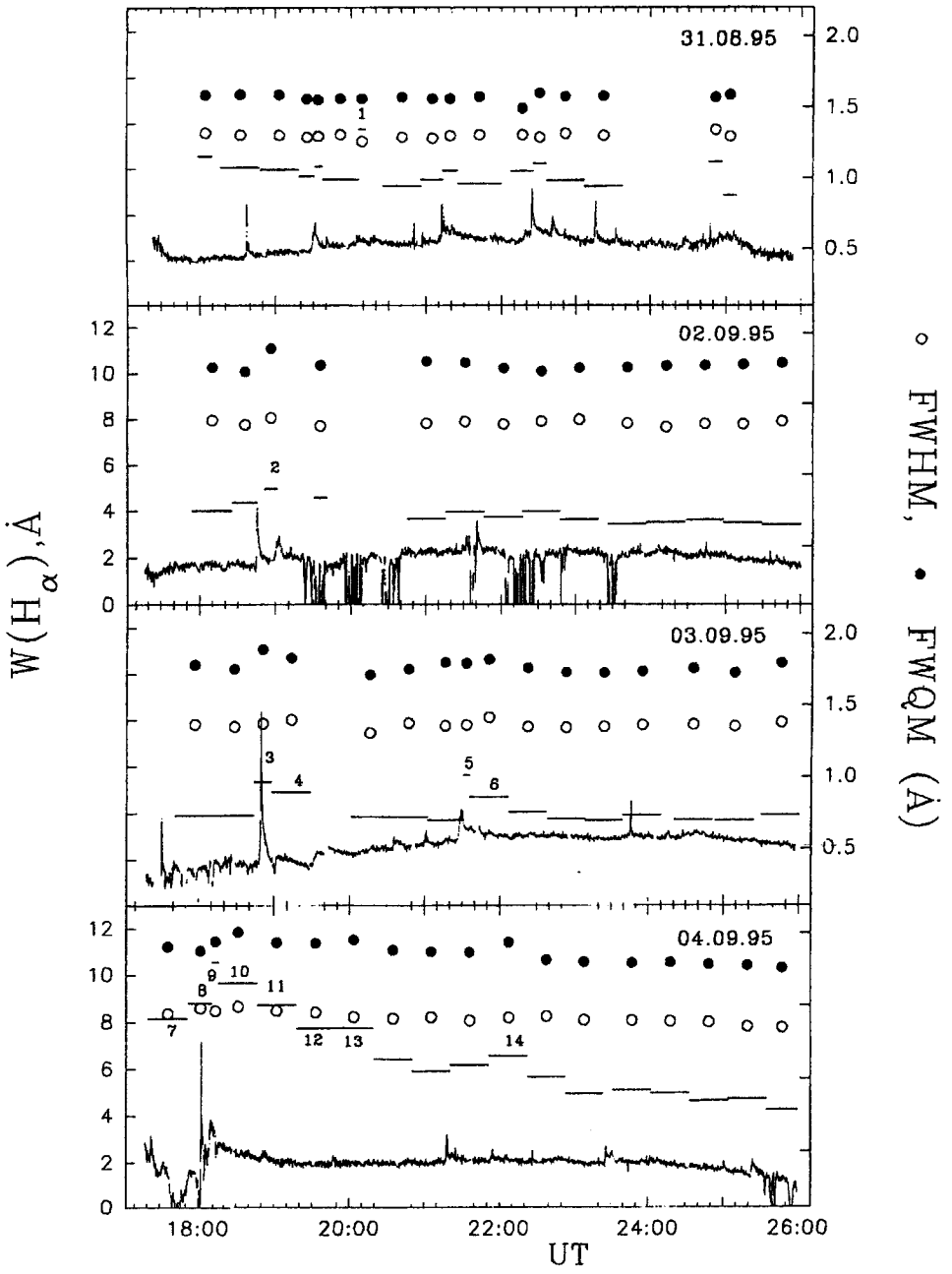

Figure 13 The U-band light curves and characteristics of H_α emission line: the horizontal lines correspond to equivalent widths, open circles indicate the full widths of the line at the level of half of maximum intensity (FWHM), and dark circles represent the full widths of the line at the level of quarter of maximum intensity (FWQM).

Table 7. Spectral characteristics of EV Lac in the active states in 1995

NN	*Date and UT of beginning and end of exposure*					*Amplitudes* $\Delta U(mag)$ *beginning*	*end*	*averaged*	W_{H_α} (Å)	$FWHM$ (Å)	$FWQM$ (Å)	W_{CaI} (Å)	$FWHM_{nar}$ (Å)	$FWHM_{wid}$	E_{wid}/E_{tot}	Δv (km/s)
1	31.8	20^h	6^m	32^s –	11^m	22^s	.06	.03	.05	7.73	1.26	1.56	0.55	1.6			
2	2.9	18	51	27 –	00	59	.09	.20	.07	4.94	1.40	1.89	0.51	2.4			
3	3.9	18	43	47 –	57	18	.04	.02	.51	5.35	1.37	1.89	0.47	3.1			
4		18	58	02 –	28	02	.02		.13	4.92	1.39	1.83	0.51	1.5			
5		21	30	35 –	35	33	.25	.11	.16	5.64	1.36	1.80	0.63	2.1			
6		21	36	11 –	06	10	.11	.01	.05	4.71	1.41	1.82	0.48	1.7			
7	4.9	17	21	18 –	51	18				8.15	1.45	1.91	0.51	1.4	5.0	0.23	49
8		17	52	51 –	10	36		.49	> .3	8.81	1.49	1.89	0.52	1.5	4.0	0.26	60
9		18	11	11 –	15	54	.49	.18	.31	10.56	1.47	1.95	0.65	1.4	4.6	0.46	22
10		18	16	31 –	46	31	.18	.05	.14	9.64	1.50	2.01	0.43	1.5	5.8	0.48	42
11		18	47	16 –	17	16	.05		.07	8.71	1.47	1.94	0.48	1.4	4.8	0.48	54
12		19	18	09 –	48	08				7.73	1.46	1.94	0.48	1.4	4.3	0.48	46
13		19	48	45 –	18	45				7.74	1.43	1.96	0.44	1.3	4.6	0.61	36
14		21	52	11 –	22	11	.00	.00	.02	6.56	1.42	1.94	0.48	1.2	4.2	0.79	−2

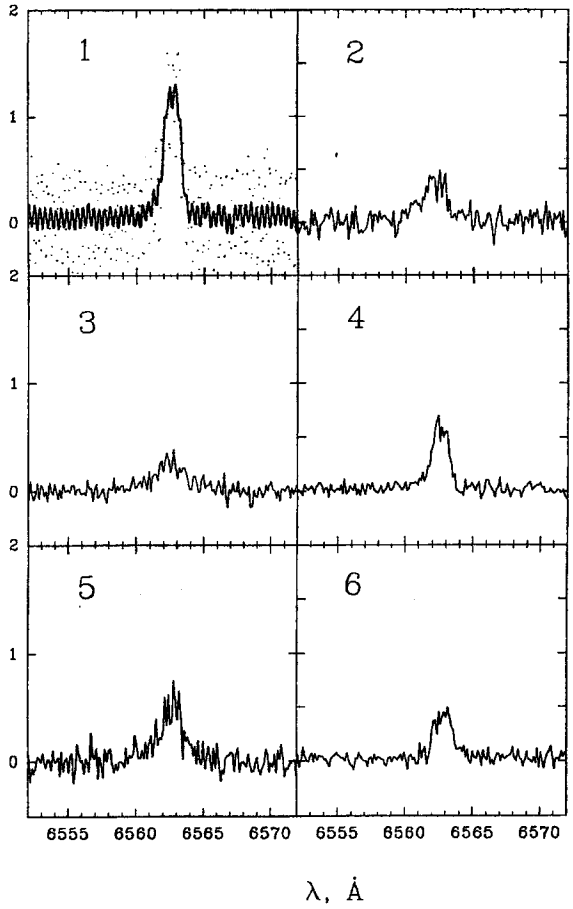

Figure 14 Profiles of pure flare radiation in the H_α line for the active state of the star: profile numbering corresponds to Figure 13.

In Table 7 quantitative characteristics of the 14 selected spectra are assembled. In the third column of the table the U-band amplitudes at the beginning of the spectral exposures, at their end and there averaged over the whole duration of the exposures are given.

In Figure 14 profiles of the pure flare radiation in the H_α, line in 14 selected spectra. are shown. They were obtained by the subtraction of an appropriate nightly averaged quiet state profile from the considered spectra. The subtraction was carried out according to relation (1), but now the factor κ was fitted so that beyond the limits of the interval $\lambda\lambda$ 6559–6566Å the sum of squares of the calculated differences was minimized. In principle, this scheme is less exact than the one applied in the 1994 analysis, since a continuous flare emission is supposed to be negligible here. The usage of this wittingly less precise scheme is caused by the

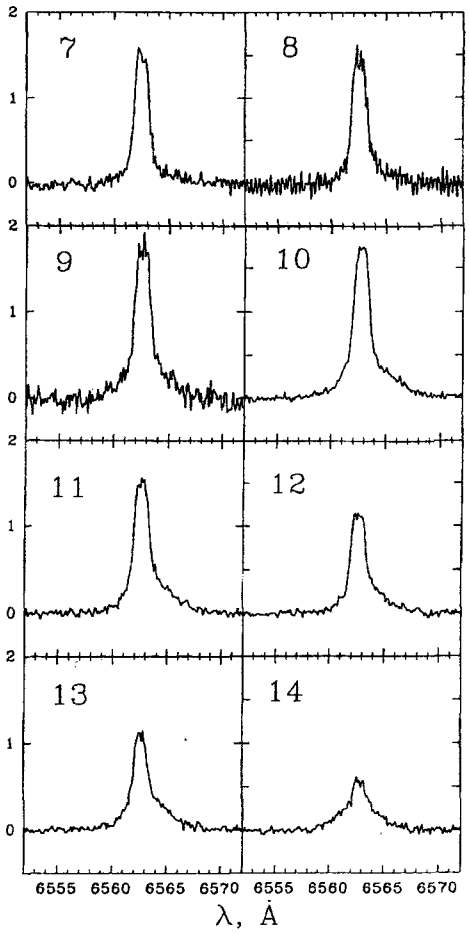

Figure 14 Continued.

absence of strong absorption details in the considered wavelength range: there are no significant intensity jumps at the heads of TiO molecular bands here and measurements of veiling of the strongest absorption line Ca I λ 6573Å do not provide the necessary accuracy for the evaluation of a flare continuum. However, in the red region of the spectrum the ratio of the intensity of flare continuum emission to the stellar continuum is much less than in the green region of the spectrum, therefore, any introduced errors should be small.

Figure 14 shows an asymmetry of some profiles of pure flare emission: in spectra NN 2 and 5 it is possible to suggest a strengthening of the "blue" wing, and in almost all spectra on September 4 (NN 7–13) a strengthening of the "red" wing is confidently observed. The profiles of the pure flare radiation can be well represented by Gaussians: for each of the rather symmetric profiles (NN 1–6) one Gaussian is

enough; for the asymmetric profiles (NN 7–13 and N 14) two Gaussians with appreciably different widths are needed. The parameters of these Gaussians are listed in the last four columns of Table 7: in columns 8 and 9 the total widths at levels of half maximum intensities of the narrow and the wide Gaussians, respectively, are presented. In column 10 the percentage of total energy within the wide components is shown and in column 11 the shifts of the centres of the wide components relative to the narrow ones are given. The table shows that these shifts, as a rule, are of several dozens km/s and that the wide Gaussians contain from 23 up to 79% of total flare emission in the line.

Estimations of the widths of various emission lines are essential for the diagnostics of radiating matter. However, making quantitative comparison of the data in Tables 5 and 7 one should take into account, that, firstly, these data refer to independent events on EV Lac and, secondly, they are obtained with different spectrographs and their instrumental widths differ by about five times. Keeping in mind these circumstances, we can note that while the systematic excess of the FWHM values of the narrow Gaussians in the H_β and H_γ profiles above the corresponding values in the H_α profiles can be attributed to the closeness of all these values to respective various instrumental widths, the FWHM values of the wide Gaussians exceed instrumental widths by several times in all cases. Thus, on the basis of the data obtained, this circumstance permits us to assert that in the EV Lac active state the characteristic broadening of the H_α line is by several times less than the broadening of the H_β and H_γ lines.

4 OBSERVATIONS OF EV LAC IN THE DECAMETRIC WAVELENGTH RANGE

4.1 Observations and Analysis of Obtained Data

As in the 1992 campaign (Abranin *et al.*, 1994; Abdul-Aziz *et al.*, 1995), in 1994 EV Lac was monitored with UTR-2 at frequencies of 20 and 25 MHz. For these observations UTR-2 was supplied with a new system of preamplifiers with essentially larger – by about 12 dB – dynamic range. The high linearity of the amplifiers with optimal distribution of amplification between the receiving elements decreased intermodulation interference significantly. The last one is known as the main restricting factor in the reception of weak signals at the decametric band, which is highly loaded by radio station interference.

Earlier we used three criteria to select probable bursts of stellar origin from terrestrial interference: (1) comparison of signals at two beams, one of which was directed towards the star and the other was shifted by about one degree in declination; (2) comparison of the time of signal arrival at different frequencies with an expected relative delay of the lower frequency due to dispersion within the interstellar medium and (3) time coincidence of radio bursts and optical flares on the star. In 1994 an additional and more effective criterion to select radio bursts from the star was applied as follows. At each frequency of observations the flux density of

the signal was measured simultaneously by two channels with essentially different antenna paterns. In the first channel the north–south and the east–west signals of UTR-2 were multiplied and gave $S_\times$, and in the second one they were added and gave S_+. The flux density of the responses of the two channels was calibrated using Cyg A, whose declination lies close to the declination of EV Lac ($\delta = 40°36'$). If the bursts were received from the direction to the star, the fluxes measured by both channels should be equal within the measurement accuracy, which is about ±30%. Otherwise they differed by several times. If interference was detected only by one of arms, in the added channel the response (S_+) appeared to be about 30 dB higher than in the multiplied one ($S_\times$).

We note that in the case of an aerial of the size of UTR-2 with ideal amplitude-phase current distribution and accounting for the fact that interference from radio stations comes from altitudes that do not exceed 15°, this difference should be of the order of several dozens. However, due to the large spread of phases and amplitudes of the currents in the vibrators and the floors of aerial phasing a rather large diffuse field is found. Therefore the far side lobes appear to be contaminated significantly by the diffuse field which leads to a reduction of the $S_+/S_\times$ ratio.

In 1994 EV Lac was monitored from 20:30 UT till 26:00 UT each night from August 26 to August 31. During this time 18 cases of increased radio emission were registered. They all were selected exclusively by the first of the above-listed criteria. However, 12 of them did not satisfy our new criterion and, hence, represented interference, received by the side lobes of the aerial.

The other six bursts, which satisfy two of our criteria (the first of the old criteria and the new criterion), are marked in Figure 1 by straight vertical lines with a linear scale of 120 Jy/mm; bursts detected at 20 MHz are marked with lines directed upward from the time axis and bursts detected at 25 MHz are marked with downward directed lines. Quantitative characteristics of these bursts are given in Table 8.

Table 8. Characteristics of the UTR-2 radio bursts selected by comparing the signals in two beams pointing at different directions

Date	*Beginning of burst (UT)*	$S_\times$ *25 MHz (Jy)*	$S_\times$ *20 (Jy)*	S_+ *25 MHz (Jy)*	S_+ *20 (Jy)*	S_+/S_x	*Duration of burst (s) 25 MHz*	*20*
26.8.94	$22^h\ 07^m\ 51^s$		170		150	0.9		10
27.8.94	22 25 34		1000		1100	1.1		6
27.8.94	22 25 54		410		540	1.3		5
27.8.94	22 26 06		1250		1400	1.1		17
28.8.94	21 39 50	150	210	150	200	1.0	10	12
28.8.94	23 12 34	2500		4000		1.6	53	

It should be emphasized that our new criterion (as well as all criteria used earlier) does not guarantee a confident identification of a signal from the star: if responses $S_\times$ and S_+. are not equal, the detected signal is certainly interference, but if $S_\times$ and S_+ are about equal, it does not represent final evidence that the

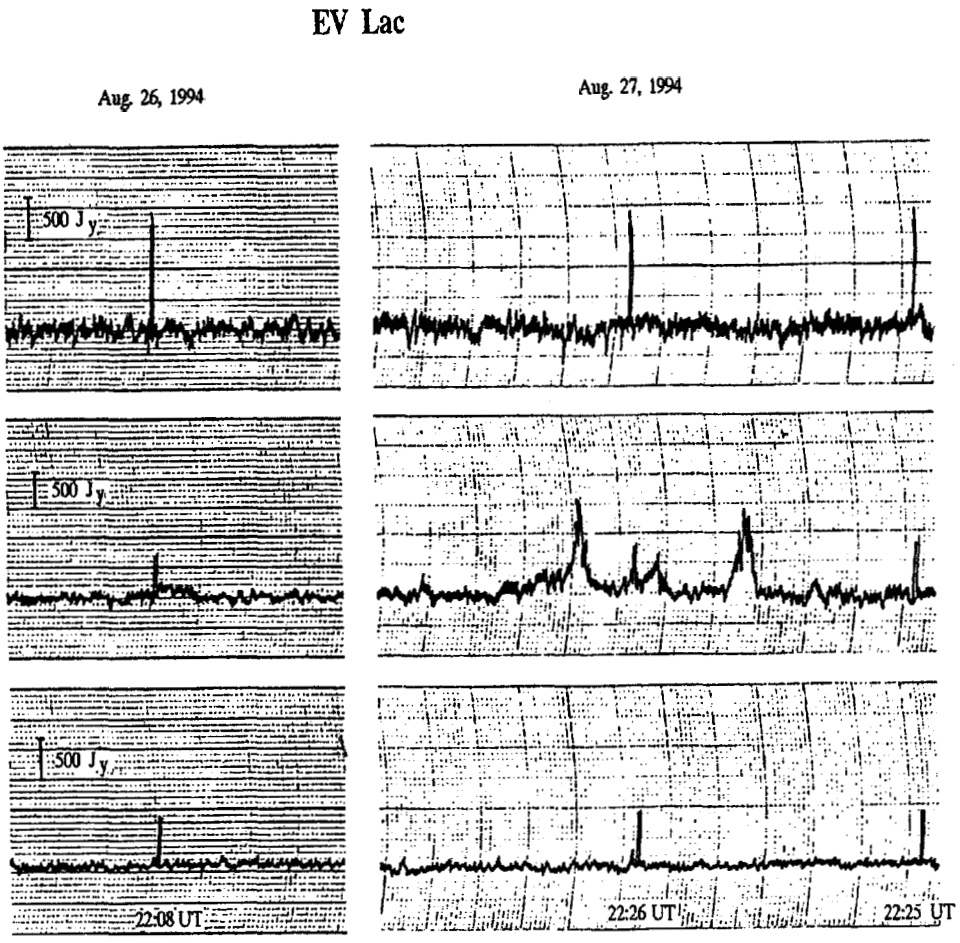

Figure 15 Decametric bursts registered by UTR-2 during the monitoring of EV Lac.

burst is received from the star by the primary lobe. A similar signal can be received casually, under some conditions, even through the side lobes.

In this respect there are serious doubts concerning the bursts on August 28. One of them – at 23:12:34 UT – gave a ratio of $S_+/S_\times = 1.6$, an appreciable difference from unity and which exceeds the errors of our measurements. This fact alone is enough to exclude this burst of stellar origin. Furthermore its temporal duration is typical for interference. Concerning criterion 3, the occurrence of this burst about 10 minutes after the optical flare – similarly to the most intense solar type II bursts – is likely to be casual.

A very weak burst was observed earlier on this night, at 21:39:57 UT, simultaneously at two frequencies, which is a rather rare event. The total duration of these bursts at zero level is about 10 s. Unfortunately, both these burst activities – espe-

cially at 25 MHz – were observed at the low limit of the radio telescope sensitivity, and in time close to the discrete switching of the aerial beams for the tracking of the star. These circumstances do not permit us to establish any reliable influence of the interstellar dispersion: their maxima are very flat. The burst at 20 MHz finished about 1 s later than that at 25 MHz. However this result is not reliable, firstly because it can be caused by a selective effect owing to the low sensitivity of the radio telescope at the time of observation; and secondly because the termination of the burst is located on the record between two consecutive time markers, which mark every minute of observations and coincide with the electrical switching of the control system of the aerial beams. Therefore it cannot be excluded that the shift between the termination of the bursts at the two frequencies is caused by the influence of the switching. This 10 s burst does not correlate with any optical flare.

Another four 20 MHz bursts were observed on August 26 and on August 27. Their temporal structures are shown in Figure 15. Unfortunately for the multiple burst on August 27 we do not have confident information, with high temporal resolution, about the optical state of the star.

Finally, the weak 20 MHz burst on August 26 at 22:08 UT – see Figure 5 – coincides well in time with a small optical flare on EV Lac. Hence, this burst satisfies the largest number of criteria in our sample and therefore it bears the highest probability of being of stellar origin.

We shall consider a possible theoretical interpretation of this event.

4.2 On the Possible Nature of Decametric Bursts from the Star

Assuming that the linear dimension of the burst region is equal to the stellar radius, $R_* = 0.35R_\odot$, the brightness temperature of the burst on August 26 at 22:08 UT at 20 MHz is estimated as 2×10^{18} K. Such a high brightness temperature requires a coherent mechanism of radiation. At higher frequencies of metre and centimetric wavelengths one usually applies the electron–cyclotron maser radiation or the plasma mechanism. These mechanisms were discussed in the interpretation of short decametric bursts, registered on EV Lac in 1992 (Abdul-Aziz *et al.*, 1995). Now it is natural to investigate whether these mechanisms can also explain decametric bursts of about 10 s duration.

Is it possible to explain the detected burst using an electron–cyclotron maser mechanism? It is usually assumed that this mechanism is realized under the availability of an electron distribution with a loss cone, i.e. the radiation should be connected to a magnetic loop (Melrose and Dulk, 1982; Dulk, 1985). Since radiation of this mechanism occurs at ω_{Be} or its harmonics, the appropriate magnetic field should be less than 10 Gs. Hence, the appropriate magnetic arches should be high enough and we shall assume $h \sim R_*$ (Bastian, 1990). Let us find the brightness temperature which it is possible to expect in this mechanism. We shall use the estimation formula of Melrose and Dulk (1982):

$$T_B = (mv_0^2/2\pi) \cdot n' \cdot (2\pi c^2/\omega v_0)^3 \tag{4}$$

where v_0 is the characteristic velocity of electrons in the loss cone which we shall assume to be 0.1 c (Melrose and Dulk, 1982); ω is the radiation frequency, equal in our case to $2\pi \cdot 20$ MHz; $n'/n \sim 10^{-4}$ is the relative density of the electrons in the loss cone; and $n = 5 \times 10^4$ cm^{-3} is the plasma density, which corresponds to the relation $\omega_{pe} \sim 0.1\omega_{Be}$. Substituting these values in equation (4), we get

$$T_B \sim 10^{20} \text{ K}. \tag{5}$$

However, this is the radiation in the impulse (Melrose and Dulk, 1982). Since the detected burst is of several seconds duration, it is necessary to restore the loss cone by reducing the brightness temperature by $\Gamma L/v_0$ times, where $\Gamma = 10^{-2}\omega$ is the rate of increase of a wave with frequency ω and $L \sim h$ is the length of a loop (Melrose and Dulk, 1982). In our case this gives $T_B = 10^{13}$ K . Thus, the electron–cyclotron maser mechanism cannot, apparently, produce the observed brightness temperature of our burst which had a duration of about 10 s.

We consider now the plasma mechanism. By its duration, the observed burst is reminiscent of type III solar bursts at decametric wavelength (Abranin *et al.*, 1980), though its brightness temperature is higher by several orders of magnitude (Melrose, 1989). Can the plasma mechanism which is succesful as a mechanism for type III solar bursts produce much higher brightness temperatures for stellar bursts? We evaluate the highest possible brightness temperature which this mechanism can give. Since the radiation source of type III solar bursts is an electron flux, the energy density of the plasma waves (Langmuir waves) can be evaluated as follows

$$W_l = n' m v_0^2 \tag{6}$$

where n' is the density of the electron flux and v_0 their characteristic velocity. Then the brightness temperature of the plasma waves can be deduced from the relation $W_l = T_l \cdot \int d\boldsymbol{k}/(2\pi)^3$. This gives

$$T_l = (1/8\pi) \cdot n' m v_0^2 \cdot (2\pi v_0/\omega)^3. \tag{7}$$

In the case of maximum efficiency for the transformation of longitudinal waves into transversal ones

$$T_t \sim T_l. \tag{8}$$

Assuming $n'/n = 10^{-4}$ and $v_0 = 10^{10}$ cm/s, we have from (7) and (8)

$$T_t = 10^{18} \text{ K}. \tag{9}$$

Since T_t depends strongly on v_0, a small increase in v_0 leads to noticeable increase of T_t. Thus, we see that the plasma mechanism, in principle, can produce brightness temperatures of the order of the observed radiation. It can originate from high magnetic arches, $h \sim R_*$, with plasma density $n = 0.5 \cdot 10^7$ cm^{-3}, as well as from regions of open magnetic force lines. If one accepts the second case, the question arises: why was radiation at 25 MHz not observed? This can be connected with the decrease of radiation intensity with growth of frequency. So for solar type III

bursts a spectral index is in the limits $\alpha = -2, \ldots, -6$ (Subramanyan *et al.*, 1993). If the same spectral index is applied to our measurement the flux density at 25 MHz would be too weak.

The decametric burst discussed above had as high a brightness temperature – about 10^{18} K – as the short bursts, described earlier by us (Abranin *et al.*, 1994; Abdul-Aziz *et al.*, 1995). However, its duration of about 10 s is essentially longer than in the earlier bursts whose temporal structure was less than 1 s. Therefore, one may conclude that this radio emission is of different type, and connected to a different radiation mechanism.

5 CONCLUSION

Among the numerous flares of EV Lac, registered in 1994 and in 1995, two flares had large amplitudes which has allowed us to carry out a quantitative analysis of their own radiation using colour–colour diagrams, covering the whole wavelength range of the *UBVRI* system. This analysis confirmed our earlier conclusion that at any phase of development of flares – their fast flaring up, at brightness maximum and during slower fading – none of the considered radiation sources – absolute black body, optically thin or thick (in the Balmer continuum) hydrogen plasma, layers of stellar atmosphere, heated up by a flux of fast particles – can present radiation of flares within the whole range of the *UBVRI* system alone. Therefore, the observations can be represented by a combination of various mechanisms or one has to develop more sophisticated models of matter radiating in flares.

Patrol observations in the K and H bands have not shown appreciable and simultaneous variations of IR stellar brightness in coincidence with the optical flares we observed. However, all flares we detected had small amplitudes, except the 1.0 mag U-band flare on 3.9.94, which showed a gradual K-band decrease following the flare maximum. Therefore, these data are not adequate to address the question of the origin of the IR light decrease during large-amplitude optical flares, as suggested by some current theoretical models of stellar flares.

Estimations of the degree of spottedness of the star were made within the framework of two various approaches. With the conventional approach, observations of only one season are used to find differential spottedness of lighter and darker hemispheres of the star. Within the framework of the recently proposed and advanced model of zonal spottedness of red dwarf stars (Alekseev and Gershberg, 1996a–c), the absolute brightness maximum of the star, which was found in long-term observations of the star, and the effects of limb–darkeninig, were taken into account. Taking into accounting certain advantages of the zonal spottedness model (Alekseev and Gershberg, 1997), one should prefer evaluations of the spottedness of EV Lac, based on this model. However, in both cases shares of the stellar surface, covered by dark spots, turned out to be tens times larger as compared to the largest appropriate share of the solar surface, detected during one and a half centuries of observations of the Sun.

An analysis of numerous EV Lac spectra in the blue-green region of the spectrum, obtained in 1994, has allowed us to evaluate changes of characteristics of H_β and H_γ emission in the active state of the star and to find additional emission lines of metals. Between the intensities of all these lines and the He I λ 4471 Å line, a rather close correlation is found. For the first time in an active state of the star, a long-lasting He II λ 4686 Å emission was found and a spliting of this line into two components was detected: the "red" component has a normal wavelength while the "blue" one was shifted by –400 km/s. The existence of this shifted component and the absence of the correlation between the He II line and lines mentioned above lead to the conclusion that He II emission is formed in another region of stellar flares.

Spectral observations of EV Lac in 1995 were carried out in the red region of the spectrum and have allowed us to evaluate variations of characteristics of H_α emission in the quiet and active states of the star. A close correlation was found between the quiet state intensity of this line and the spottedness of the star. The appearance of asymmetry of the H_α line profiles during flares is confirmed, "red" wing enhancements are stronger and more frequent than "blue" ones. During stellar activity short-lived wide components can be detected in Balmer line profiles, which in H_β and H_γ profiles are several times wider than in H_α profiles, but broad components of H_α seem to be more durable than there of H_β and H_γ.

In 1994 EV Lac was monitored with UTR-2 at the decametric wavelength range during 33 hours. 18 radio bursts were registered; four criteria to select bursts of a non-terrestrial nature were applied to them. As a result the burst on 26.8.94 at 22:08 UT was selected as one of probable stellar origin. Its duration is about 10 s, it coincides with the optical flare with $\Delta U = 0^m.5$, and satisfies the majority of the radio criteria of selection and is connected with the stellar activity with the highest probability. This event with brightness temperature of about 10^{18} K, apparently, can be explained within the framework of the plasma mechanism of radiation.

Acknowledgements

The spectral research in 1995 described in this publication was made possible in part by Grants R2Q000, R2Q200, U1C00 and U1C200 from the International Science Foundation and by Grant A–05–067 from the ESO C & EE Programme. The radio research described in this publication was made possible in part by Grants NU9 W000 and NU9 W200 from the International Science Foundation. The Italian group should like to thank the Italian *Ministero dell'Universitá e della Ricerca Scientifica e Tecnologica* for continuous support to the *Stellar Activity research program* carried out at the Catania Astrophysical Observatory. Our thanks to Mrs. A. V. Terebizh for help in preparation of the manuscript.

References

Abdul-Aziz, H., Abranin, E. P., Alekseev, I. Yu., Avgoloupis, S., Bazelyan, L. L., Beskin, G. M., Brazhenko, A. I., Chalenko, N. N., Cutispoto, G., Fuensalida, J. J., Gershberg, R. E., Kidger, M. R., Leto, G., Malkov, Yu. F., Mavridis, L. N., Pagano, I., Panferova, I. P.,

Pustil'nik, L. A., Rodonò, M., Seiradakis, J. H., Sergeev, S. G., Spencer, R., Shakhovskaya, N. I., and Snakhovskoy, D. N. (1995) *Astron. Astrophys. Suppl. Ser.* **114**, 509.
Abranin, E. P., Bazelyan, L. L., Rapoport, V. O., and Tsybko, Ya. G. (1980) *Solar Phys.* **66**, 333.
Abranin, E. P., Alekseev, I. Yu., Bazelyan, L. L., Brazhenko, A. I., Gershberg, R. E., and Shakhovskaya, N. I. (1994) *Kinematics and Physics of Celestial Bodies* **10**, 70.
Alekseev, I. Yu., Gershberg, R. E., Ilyin, I. V., Shakhovskaya, N. I., Shakhovskoy, N. M., Avgoloupis, S., Mavridis, L. N., Seiradakis, J. H., Kidger, M. R., Panferova, I. P., and Pustil'nik, L. A. (1994) *Astron. Astrophys.* **288**, 502.
Alekseev, I. Yu. and Gershberg, R. E. (1996a) *Astron. Reports* **73**, 589.
Alekseev, I. Yu. and Gershberg, R. E. (1996b) *Astron. Reports* **73**, 579.
Alekseev, I. Yu. and Gershberg, R. E. (1996c) *Astrofizika* **39**, 67.
Alekseev, I. Yu. and Gershberg, R. E. (1997) *Astron. Reports* **74**, 240.
Bastian, T. S. (1990) *Solar Phys.* **130**, 265.
Berdyugin, A. V., Gershberg, R. E., Ilyin, I. V., Malanushenko, V. P., Shakhovskaya, N. I., Shakhovskoy, N. M., Pagano, I., Panferova, I. P., and Pustil'nik, L. A. (1995) *Izvestiya Krymsk. Astrophys. Obs.* **89**, 81.
Berezin, V. Yu., Zuev, A. G., Kiryan, G. V., Rybakov, M. I., Khvilitisky, A. T., Ilyin, I. V., Petrov, P. P., Savanov, I. S., and Shcherbakov, A. G. (1991) *Letters to Sov. Astron.* **17**, 953.
Bopp, B. W. and Moffett, T. J. (1973) *Astrophys. J.* **185**, 239.
Byrne, P. B. and Gary, D. E. (1989) In: B. M. Haisch and M. Rodono (eds.), *Solar and Stellar flares*, IAU Coll. No. 104, Poster papers, Catania Astrophys. Obs. Special Publ., p. 63.
Doyle, J. G. and Byrne, P. B. (1987) In: J. L. Linsky and R. E. Stencel (eds.), *Cool Stars, Stellar Systems, and the Sun*, Proc. 5th Cambridge workshop, Boulder, July 7–11, 1987, Lecture Notes in Physics **291**, 173.
Dulk, G. A. (1985) *Ann. Rev. Astron. Astrophys.* **23**, 169.
Gershberg, R. E. and Chugainov, P. F (1966) *Sov. Astron.* **43**, 1168.
Gershberg, R. E. and Chugainov, P. F. (1967) *Sov. Astron.* **44**, 260.
Gershberg, R. E., Grinin, V. P., Ilyin, I. V., Nesterov, N. S., Shakhovskaya, N. I., Getov, R. G., Ivanova, M. S., Panov, K. P., Tsvetkov, M. K., Tsvetkova, A. G., and Leto, G. (1991a) *Astron. Zh. (Sov. Astron.)* **68**, 548.
Gershberg, R. E., Ilyin, I. V., and Shakhovskaya, N. I. (1991b) *Astron. Zh. (Sov. Astron.)* **68**, 959.
Gershberg, R. E., Ilyin, I. V., Rostopchina, A. N., Shakhovskaya, N. I., Garbuzov, G. A., Pettersen, B. R., Korhonen, T., Avgoloupis, S., Mavridis, L. N., Seiradakis, J. H., Konstantinova-Antova, R. K., Antov, A. P., Melkonyan, A. S., Panferova, I. P., Pustil'nik, L. A., Herouni, P. M., and Oskanyan, A. V. (1993) *Astron. Reports* **70**, 984.
Greenstein, J. L. and Arp, H. (1969) *Astrophys. Lett.* **3**, 149.
Joy, A. H. (1945) *Astrophys. J.* **102**, 168.
Joy, A. H. and Humason, M. L. (1949) *Publ. Astron. Soc. Pacific* **61**, 133.
Kunkel, W. E. (1970) *Astrophys. J.* **161**, 503.
Mavridis, L. N., Asteriadis, G., and Mahmoud, F. M. (1982) In: E. G. Mariolopoulos, P. S. Theocaris, and L. N. Mavridi (eds.), *Compendium in Astronomy*, Reidel, Dordrecht, 253.
Melrose, D. B. (1989) *Solar Phys.* **120**, 369.
Melrose, D. B. and Dulk, G. A. (1982) *Astrophys. J.* **259**, 844.
Mochnacki, S. W. and Schommer, R. A. (1979) *Astrophys. J.* **231**, L77.
Moffett, T. J. and Bopp, B. W. (1976) *Astrophys. J. Suppl. Ser.* **31**, 61.
Piirola, V. (1984) *Observ. Astrophys. Lab. Univ. Helsinki Report*, No. 6, 151.
Severny, A. B., Steshenko, N. V., and Khokholova, V. L. (1960) *Astron. Zh. (Sov. Astron.)* **37**, 23.
Subramanian, K. R., Gopalswami, N., and Sastry, Ch. V. (1993) *Solar Phys.* **143**, 301.
Tandberg-Hanssen, E. (1963) *Astrophys. J.* **137**, 26.